Cycling of oxyanion-forming trace elements in groundwaters from a freshwater deltaic marsh

Katherine Telfeyan [a, *, 1], Alexander Breaux [a, b], Jihyuk Kim [c], Alexander S. Kolker [b, a], Jaye E. Cable [c], Karen H. Johannesson [a]

[a] Department of Earth and Environmental Sciences, Tulane University, New Orleans, LA, 70118, USA
[b] Louisiana Universities Marine Consortium, Chauvin, LA, 70344, USA
[c] Department of Marine Sciences, University of North Carolina at Chapel Hill, Chapel Hill, NC, 27514, USA

ARTICLE INFO

Article history:
Received 11 October 2017
Received in revised form
11 February 2018
Accepted 22 February 2018
Available online 2 March 2018

ABSTRACT

Pore waters and surface waters were collected from a freshwater system in southeastern Louisiana to investigate the geochemical cycling of oxyanion-forming trace elements (i.e., Mo, W, As, V). A small bayou (Bayou Fortier) receives input from a connecting lake (Lac des Allemands) and groundwater input at the head approximately 5 km directly south of the Mississippi River. Marsh groundwaters exchange with bayou surface water but are otherwise relatively isolated from outside hydrologic forcings, such as tides, storms, and effects from local navigation canals. Rather, redox processes in the marsh groundwaters appear to drive changes in trace element concentrations. Elevated dissolved S(-II) concentrations in marsh groundwaters suggest greater reducing conditions in the late fall and winter as compared to the spring and late summer. The data suggest that reducing conditions in marsh groundwaters initiate the dissolution of Fe(III)/Mn(IV) oxide/hydroxide minerals, which releases adsorbed and/or co-precipitated trace elements into solution. Once in solution, the fate of these elements is determined by complexation with aqueous species and precipitation with iron sulfide minerals. The trace elements remain soluble in the presence of Fe(III)- and SO_4^{2-}- reducing conditions, suggesting that either kinetic limitations or complexation with aqueous ligands obfuscates the correlation between V and Mo sequestration in sediments with reducing or euxinic conditions.

1. Introduction

Deltaic wetlands are important sites for carbon cycling and ecosystem productivity and provide a barrier for inland communities against storms (Chmura et al., 2003; Day et al., 2007; Kemp et al., 2014). Owing to their dynamic nature, deltaic wetlands are sensitive recorders of changing hydrologic regimes, anthropogenic influence, and sea level rise (Paola et al., 2011). Particularly important is their function as a filter for anthropogenic contaminants between upland regions and the ocean (Windom et al., 1989; Alewell et al., 2008). The biogeochemical reactions that occur within deltaic wetlands can ultimately impact marine biogeochemistry and fluxes of constituents to the ocean (Bianchi and Allison, 2009). Although many studies have focused on the influence of large river fluxes to the ocean (e.g., Martin and Whitfield, 1983; Shiller and Boyle, 1987; Bianchi and Allison., 2009) or the biogeochemistry of shallow pore waters (e.g., Kostka and Luther, 1995; Sundby et al., 2003), much less is known about biogeochemical processes at depth in deltaic marsh systems and how these processes may affect fluxes of constituents to the coast (Beck et al., 2008).

In this study we focus on the biogeochemical cycling of redox sensitive trace elements (i.e., Fe, Mn, Mo, W, As, V) in marsh groundwaters exchanging with an interdistributary lake of the Mississippi River Delta system. The fate of these trace elements in coastal systems has important consequences for biological cycles, potential contamination in the environment, and because of their redox sensitivity, their use in paleoredox reconstructions in paleoceanographic studies (Bone et al., 2006; O'Connor et al., 2015). Owing to the seasonal variation in redox reactions, cycling of trace elements is dynamic, and concentrations are representative of

* Corresponding author.
E-mail address: ktelfeya@tulane.edu (K. Telfeyan).
[1] Earth and Environmental Sciences Division, Los Alamos National Laboratory, Los Alamos, NM, 87545 USA.

https://doi.org/10.1016/j.ecss.2018.02.024

numerous processes, including biologically mediated redox reactions, adsorption/desorption reactions, and ion-exchange reactions occurring within the marsh system. For example, in natural dilute oxic waters, Mo and W occur as fully deprotonated oxyanions in the hexavalent state (MoO_4^{2-}, WO_4^{2-}), whereas V and As exist as hydrolyzed oxyanions in the pentavalent state, where the degree of protonation depends on pH (e.g., $H_2VO_4^-$, HVO_4^{2-}, $H_2AsO_4^-$, $HAsO_4^{2-}$; Cruywagen, 2000; Smedley and Kinniburgh, 2002; Wright and Belitz, 2010; Gustafsson, 2003). As oxyanions, desorption from mineral surfaces occurs at alkaline pH where mineral surface charges become increasingly negative (Hingston et al., 1967; Stumm and Morgan, 1996). Adsorbed oxyanions will also be released to solution upon reductive dissolution of Fe(III)/Mn(IV) oxide/oxyhydroxide host phases (Davison, 1993; Lovley, 1987).

Under sulfate reducing conditions, the production of dissolved sulfide can also influence the speciation and reactivity of these trace elements as S(-II) can act as both a reducing agent or complexing ligand (Clarke and Helz, 2000; Erickson and Helz, 2000; Planer-Friedrich et al., 2007; Mohajerin et al., 2014). For example, vanadate can be reduced by H_2S to the more particle reactive V(IV) or V(III) oxidation states, leading to decreasing aqueous concentrations (Wanty, 1986; Breit and Wanty, 1991), whereas under sulfate reducing conditions, Mo, W, and As are converted to thioanions with or without reduction (Cullen and Reimer, 1989; Erickson and Helz, 2000; Vorlicek et al., 2004; Planer-Friedrich et al., 2007; Dahl et al., 2013; Mohajerin et al., 2014). Less described but equally important is the role of organic matter affecting the solubility of these trace elements through complexation or adsorption processes (e.g., Wehrli and Stumm, 1989; Tribovillard et al., 2006; Koutsospyros et al., 2006). Polymeric forms of Mo, W, and V also exist but are negligible at the typically low metal concentrations (i.e., nanomolal, picomolal) and circumneutral pH values observed in most natural waters (Baes and Mesmer, 1976; Wesolowski et al., 1984; Wanty and Goldhaber, 1992; Cruywagen, 2000).

Detailed studies of trace element cycling in marsh groundwaters (1–6 m depth) are lacking, especially in Mississippi River Delta groundwaters, and to the best of our knowledge there have been no investigations of trace element cycling between deeper groundwaters and surface waters in the Mississippi River Delta region. Consequently, we sampled groundwaters and surface waters at an interdistributary freshwater deltaic lake (i.e., Lac des Allemands) over the course of a year to investigate processes that control trace element cycling in the system. Trace element concentrations are discussed within the context of redox chemistry of the marsh and comparison with nearby surface water samples. We highlight the importance of competition between redox processes acting to release or sequester trace elements in the sediments and complexation with dissolved ligands, which can act to increase the effective solubility of some of the studied trace elements, while enhancing the removal of others from solution.

2. Study site

The study site is located at Lac des Allemands, an interdistributary lake in the Mississippi River Delta (Fig. 1). The Mississippi River Delta formed by a series of river avulsion events beginning ~7000 years ago and built around 25,000 km^2 of river deposits with each of the 6 lobes observable today (Fisk et al., 1954; Roberts, 1997). Upon abandonment of a lobe, fine-grained deposits associated with interdistributary bays, tidal flats and marshes overlaid the coarser-grained river deposits (Coleman, 1988; Seybold et al., 2007). The Lac des Allemandes systems lies between Bayou LaFourche, which was the main channel of the Mississippi River from about 1300 years before present to about 500 years before present, and the modern mainstem of the Mississippi River. During this period, the region accumulated a complex stratigraphy of organic matter, as well as fine and coarse-grained material, with each depositional facies related to the proximity of the outlet and crevasses in the Mississippi River (Kosters et al., 1987; Tornqvist et al., 1996; Roberts, 1997). Lac des Allemands is hydrologically connected to the southern portions of Barataria Basin by Bayou des Allemands (Fig. 1A). Barataria Basin is presently under a transgressive phase, experiencing subsidence, saltwater intrusion, and erosion (Kosters et al., 1987; Kolker et al., 2013; Couvillion et al., 2011; Roberts, 1997). Furthermore, anthropogenic levee structures that constrain Mississippi River flow in the southern Mississippi River Delta prevent future river migration and land building by overbank flow. Consequently, the adjacent sediment-starved wetlands in the southern portion of the basin are left vulnerable to sea level rise and storm surge inundation (Reed, 2002). Lac des Allemands is also considered to lie within the “industrial corridor” of the delta that includes abundant industrial facilities and a number of Superfund waste sites (Catallo et al., 1995).

The region surrounding Lac des Allemands is classified as freshwater marsh, and the marsh is dominated by freshwater spikerush species, such as *Panicum hemitomon* (maidencane), *Typha latifolia*, and *Eleocharis macrostachya Britton* (Kosters et al., 1987; CRMS). There are no surface water sources to the upper Barataria Basin, although the Davis Pond Diversion opens to Lakes Salvador and Cataouatche to the south of Lac des Allemands (Fig. 1A). Precipitation is the main surface water input, of which about 40% is available for runoff (Inoue et al., 2008, and references therein). Runoff from agricultural and industrial areas accumulates nutrients, which may then accumulate in the lake. Lac des Allemands is a hypereutrophic and fresh lake, with salinities below 0.5 ppt (Ren et al., 2009). Lac des Allemands waters are considered to be N-limiting, and the cyanobacteria species *Anabaena* spp., *Anabaenopsis* spp., *Cylindrospermopsis raciborskii* spp., and *Aphanizomenon* spp. constitute the predominant phytoplankton species within the lake. The depth of Lac des Allemands ranges between 2 and 3 m and is therefore likely a polymictic lake (Ren et al., 2009).

3. Methods

3.1. Field methods

A number of small bayous extend from the lake and terminate in the adjacent wetlands (Fig. 1B). We focused on Bayou Fortier, which is the largest and most northern of these bayous because it extends north to near the natural levee of the Mississippi River and within 5.4 km of the river (Fig. 1C). Six piezometers (W1–W6) were installed in September 2013 along Bayou Fortier using vibracoring techniques (Lanesky et al., 1979). A marsh fire the following winter cleared enough vegetation to allow the installation of three additional piezometers farther inland (W7–W9; Fig. 1C). Piezometer W4 is the closest to the Mississippi River and is located within the cypress swamp near the northern reach of Bayou Fortier (Fig. 1C). Additionally, a piezometer was installed on farmland in Edgard, Louisiana (EDG), directly north of Bayou Fortier and 0.88 km south of the Mississippi River, and two piezometers were installed at different depths (183 cm and 488 cm) along the western edge of Lac des Allemands on farmland in the town of Vacherie, LA (Fig. 1B). These “farmland cores” were taken using a Geoprobe® technical drilling machine, and the piezometers were emplaced in the resulting boreholes. All piezometers were constructed from PVC pipes connected to a PVC Well Point that contained a 0.91 m screened interval. In addition to the groundwater samples collected from the piezometers, surface water samples were collected from Bayou Fortier as well as Lac des Allemands (Fig. 1B). Additionally, a

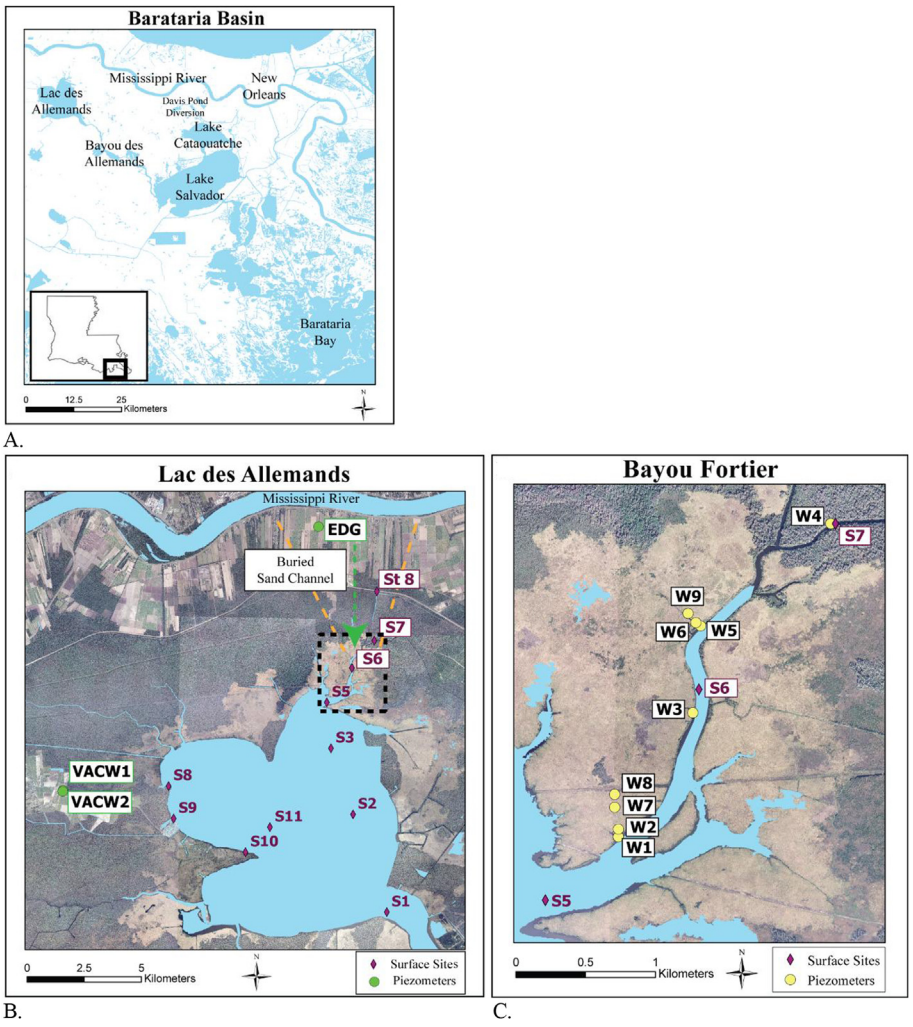

Fig. 1. A. Map of Barataria Basin in the Mississippi Delta region of southern Louisiana. **B.** Map of Lac des Allemands. Surface sites are labeled as magenta diamonds and piezometers installed on farmlands are labeled as green circles. The orange dashed line indicates the region of a buried sand unit that extends from the Mississippi River levee to the head of Bayou Fortier, and the green dashed arrow indicates the hypothesized direction of groundwater flow. The black dashed line outlines inset **C**. Map of Bayou Fortier. Marsh piezometers are labeled as yellow circles and surface sites as magenta diamonds. Maps constructed using high resolution ortho imagery downloaded from USGS Earth Explorer for input into ArcGIS. Location details for the sample sites are listed in Appendix A. (For interpretation of the references to colour in this figure legend, the reader is referred to the Web version of this article.)

surface water sample was also collected at a bayou (St 8) along LA route 3127 located 3.4 km south of the Mississippi River and 2 km north of Lac des Allemands piezometer W4 (Fig. 1B). Cores collected from Lac des Allemands sample W4 and all three of the farmland cores reveal coarse-grained sediments at depth in contrast to the very fine-grained organic-rich units constituting the remaining Lac des Allemands samples (W1-3, W5-9; Fig. 2).

Surface water samples were collected April, May, July and September of 2013 and in February, April, May, and September of 2014. Groundwater samples from the marsh piezometers were collected October of 2013 and again in February, April, May, and September of 2014 (Appendix A). Groundwater samples from the piezometers on farmland (VACW1, VACW2, and EDG) were sampled during the May and September sampling campaigns of 2014. All sampling equipment used to collect water samples was cleaned prior to sampling according to trace-metal clean procedures, and sample bottles were rinsed three times prior to collection with filtered sample water (e.g., Johannesson et al., 2004). Surface water samples were collected just below the bayou and lake surface using a peristaltic pump with Teflon® tubing attached to a 0.45 μm Gelman Sciences (polysulfone ether membrane) in-line filter. Groundwater samples were similarly sampled using a peristaltic pump after measuring depth to water level. Approximately 30 mL of filtered water sample was passed through anion exchange columns (Biorad prefilled AG® 1-X8 Resin converted to acetate form) in order to separate As(V) and As(III) species. At neutral pH and oxic to ferruginous conditions, As(V) occurs as the ionized, arsenate oxyanion (e.g., $H_2As^VO_4^-$ and $HAs^VO_4^{2-}$) and is therefore retained on the column, whereas As(III) occurs as fully protonated arsenic acid (i.e., $H_3As^{III}O_3^0$), which because it is a neutral species, passes through the column to be collected in a pre-cleaned HDPE bottle (Ficklin, 1983; Wilkie and Hering, 1998). Total As(III) is measured in this eluted fraction, and total As is measured from a separate fraction, both by sector-field ICP-MS as described below (sec. 3.2). Total As(V) is then determined as the difference between As_{Total} and As(III) (Wilkie and Hering, 1998; Haque and Johannesson, 2006). Total As(III) is assumed to consist of both As(III) bound with O as an

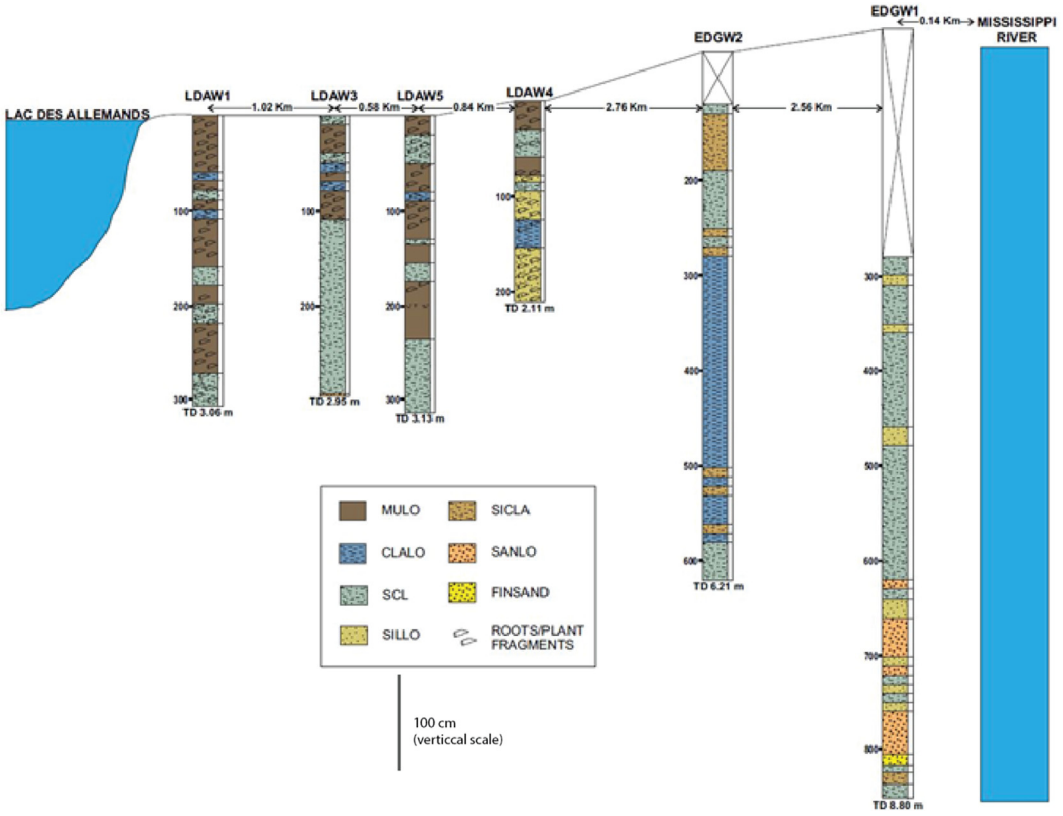

Fig. 2. Schematic cross section from Lac des Allemands to the Mississippi River with core profiles from Breaux (2015). The Lac des Allemands cores shown are the samples closest to the bayou edge (W1,W3,W5, W4). Abbreviations: MULO: muddy loam, SICLA: silty clay, CLALO: clay loam, SANLO: sandy loam, SCL: silty clay loam, FINSAND: fine sand, SILLO: silty loam.

oxyanion and As(III) bound with S as a thioanion. Similarly, total As(V) is assumed to consist of both the arsenate oxyanion and thioarsenate. This approach is imperfect because thioarsenite species may also bind to the anion-exchange column and lead to underestimation of As(III) species (Jay et al., 2004; Yang et al., 2015), but without the ability to immediately measure speciation with HPLC (e.g., Planer-Friedrich et al., 2007), this is the most accurate method.

Filtered samples were acidified with ultrapure HNO_3, chilled with ice in the field and transferred to a refrigerator at Tulane University where they were stored at 4 °C until analysis. Field blanks and duplicates were collected to control for contamination and to evaluate reproducibility during sample and analysis. Trace element analysis of the major cation and trace element samples was completed within two weeks of sample collection.

A YSI handheld multiparameter sonde was used to measure temperature, salinity, conductivity, and dissolved oxygen, and an Oakton® meter was used to measure pH. Alkalinity was determined by titration (Hach method 8203) using phenolphthalein and bromocresol green-methyl red indicators and 0.16 Eq L^{-1} or 1.6 Eq L^{-1} H_2SO_4. Total iron, Fe(II), S(-II), and SO_4^{2-} were determined using a portable Hach DR 2800 UV-VIS spectrophotometer. The FerroVer® method was used to determine total iron and the 1,10-phenanthroline method to determine Fe(II) (detection limits 0.36 μmol kg^{-1}; Eaton et al., 1995a). Ferric iron was determined as the difference between Fe_{Total} and Fe(II). Sulfate was determined by the SulfaVer® method (detection limit 0.02 mmol kg^{-1}; Eaton et al., 2005), and S(-II) was measured using the methylene blue method (detection limit 0.31 μmol kg^{-1}; Eaton et al., 1995b), which is based on Cline (1969).

3.2. Major cation and trace element analysis

The concentrations of a suite of major cations and trace elements were determined using a Thermo Fisher Element II high resolution (magnetic sector) inductively coupled plasma mass spectrometer (HR-ICP-MS). Major ions (Na, Mg, K, Ca, Sr, Ba) were diluted 100- to 10,000-fold with 2% (v/v) ultrapure HNO_3 (Optima grade) before introduction to the HR-ICP-MS for quantification. The trace elements were measured in separate runs on undiluted aliquots of each water sample. We monitored ^{88}Sr, ^{138}Ba, ^{95}Mo, ^{182}W, and ^{23}Na in low resolution mode and corrected for instrumental drift using a Re spike (220.2 nmol kg^{-1}) as the internal standard. Additionally, ^{51}V, ^{55}Mn, ^{56}Fe, ^{27}Al, ^{24}Mg, and ^{44}Ca were monitored under medium resolution, and ^{75}As and ^{39}K were monitored in high resolution mode to distinguish from potential $ArCl^+$ and ArH^+ interferences, respectively (Olesik, 2014). A Sc spike (222.4 nmol kg^{-1}) was used as the internal standard for both medium and high resolution analyses. Calibration standards were made in concentrations ranging from 5 ng kg^{-1} to 2.5 mg kg^{-1} from SPEX CertiPrep® ICP-MS Multi-Element Solution 2 in 2% HNO_3. Tungsten and Mo standards were made separately from SPEX CertiPrep® W and Mo standards, respectively. Due to instabilities in low resolution mode during analysis, W and Mo data are unavailable for the September sampling event. The accuracy of each analysis was checked using calibration check standards and a suite of certified reference material. Percent error using check standards and certified reference material is less than 20% and generally less than 10%. Although W concentrations are not reported for SLRS-4 and SLEW-3, Mohajerin et al. (2016) and Yeghicheyan et al. (2001) report W concentrations of ~70 pmol/kg for SLRS-4. We

did not detect W in the SLRS-4 standard but measured relatively constant W concentrations in the SLEW-3 standard (average ± σ = 34 ± 7 pmol/kg). Detection limits were calculated as three times the standard deviation of the blank, where the standard deviation was calculated from the blank concentrations for all analyses (Appendix B).

3.3. Geochemical modeling

Geochemical modeling was conducted using the Spec8 and React programs of Geochemist's Workbench® (version 9.0; Bethke, 2008) to calculate the thermodynamically stable dissolved species and mineral saturation states. The default thermodynamic database (Lawrence Livermore National Laboratory Database; Delany and Lundeen, 1990) was modified for As, Mo, and W to include sulfidation reactions by incorporation of data from Helz and Tossell (2008), Erickson and Helz (2000), and Mohajerin et al. (2014), respectively, as described by Yang et al. (2015). Thiomolybdate and thiotungstate formation constants have been determined experimentally by Erickson and Helz (2000) and Mohajerin et al. (2014), respectively. The sulfidation reactions for As, however, are estimated from *ab* initio computations, and although this dataset is preliminary, it provides the most current dataset available (Helz and Tossell, 2008). In addition to the sulfidation reactions, the modified database of As speciation includes dissociation constants of arsenous and arsenic acids (Nordstrom et al., 2014) and solubility constants for As-bearing minerals from Webster (1990), Eary (1992), Nordstrom and Archer (2003), and Nordstrom et al. (2014). We assumed that all measured As(III) was available for sulfidation reactions to form thioarsenite and all calculated As(V) was available to form thioarsenate species in the modeling (Yang et al., 2015). As mentioned above, this approach suffers from the potential interaction of thioarsenites with the column. However, without sulfur speciation data, specifically, quantification of zero-valent sulfur, it is not possible to systematically model As speciation between As(III) and As(V) species using the total dissolved As concentration (Helz et al., 2014). With these limitations acknowledged, the model is capable of predicting As redox and thioanion

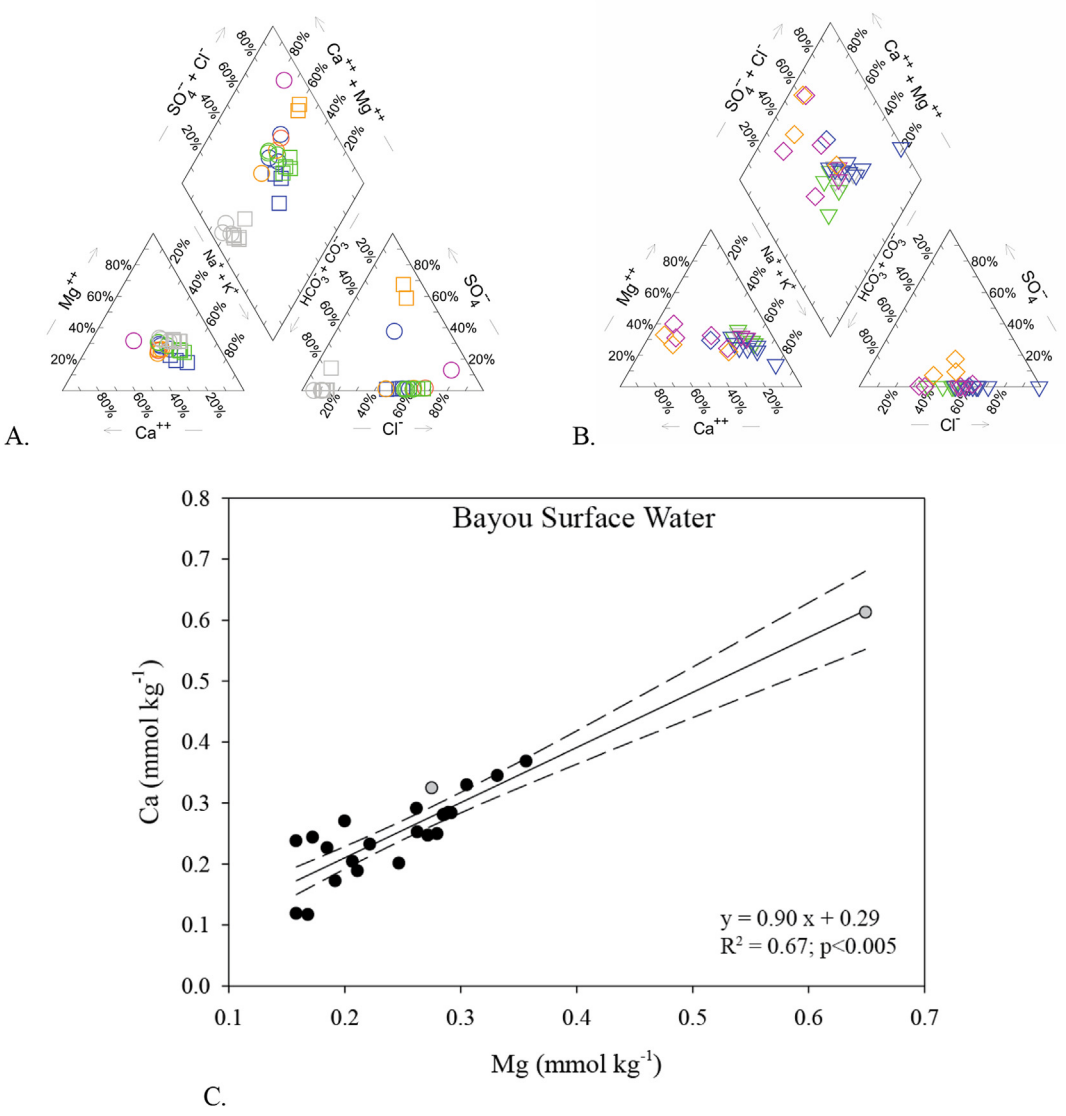

Fig. 3. Piper diagram of surface (A) and groundwaters (B). Shapes indicate sample location. Circles: bayou surface water, squares: lake surface water, triangles: groundwaters from fine-grained sediment, diamonds: groundwaters from coarse-grained sediment. Colors indicate time. Grey: October, green: February, blue: April, magenta: May, orange: September. C. Linear relationship between Mg and Ca concentrations in Bayou surface water (samples S5, S6, and S7). Upper and lower 95% confidence intervals are plotted as dashed lines. Mississippi River samples are plotted as grey symbols. (For interpretation of the references to colour in this figure legend, the reader is referred to the Web version of this article.)

formation at the order of magnitude level in Lac des Allemands waters and therefore broadens our ability to understand As cycling in these waters (Yang et al., 2015). The database also includes the solubility data for the iron sulfide minerals, mackinawite and greigite, taken from Rickard et al. (2006) and Morse et al. (1987), respectively, in addition to a possible Fe–Mo–S mineral species of the form $FeMo_{0.6}S_{2.8}$ proposed by Helz et al. (2011). Recent work suggests that the hexavalent Mo in this species may be partially reduced, but the effects on the resulting equilibrium constant are negligible in shallow sediment pore waters (Helz et al., 2014; Mohajerin et al., 2016).

4. Results

4.1. General geochemistry of surface waters and groundwaters

Hydrogeochemical facies for surface waters and groundwaters are presented on Piper diagrams to classify the waters based on relative proportions of major cations and anions (Fig. 3A and B; Santos et al., 2008). The major ion data are consistent with interpretations that groundwater derived from the Mississippi River is transported through a buried sand channel and discharges at the head of Bayou Fortier in the vicinity of surface site S7 (Kim, 2015). In particular, the bayou surface waters plot in a more Ca^{2+} enriched region than the lake surface waters, reflecting input from the Mississippi River, which is enriched in Ca^{2+} relative to the lake surface waters (Appendix C; Fig. 3A). Furthermore, Swarzenski et al. (2008) demonstrate that water derived from the Mississippi River has a constant Ca–Mg ratio, and Fig. 3C shows that the bayou waters show a significant correlation between Ca and Mg with Mississippi River water samples. The major cation data is therefore consistent with groundwater derived from the Mississippi River discharging at the head of Bayou Fortier and subsequent dilution of this water upon mixing in Lac des Allemands.

The major ion composition of the groundwaters suggests that there is hydrological communication between the bayou and the marsh groundwaters (Fig. 3A and B). Specifically, Lac des Allemands groundwaters contain low SO_4^{2-} concentrations and comparable proportions of HCO_3^- and Cl^- to the surface waters. The cation data, however, are more scattered. For example, although the groundwater samples have relatively constant proportions of Mg^{2+}, the relative proportions of Na^+ and Ca^{2+} are variable (Fig. 3B). More specifically, the groundwater samples from the farmland piezometers and Lac des Allemands piezometer W4, are enriched in Ca^{2+} relative to the other samples, suggesting greater hydrological influence from the Mississippi River. The major cation data imply that

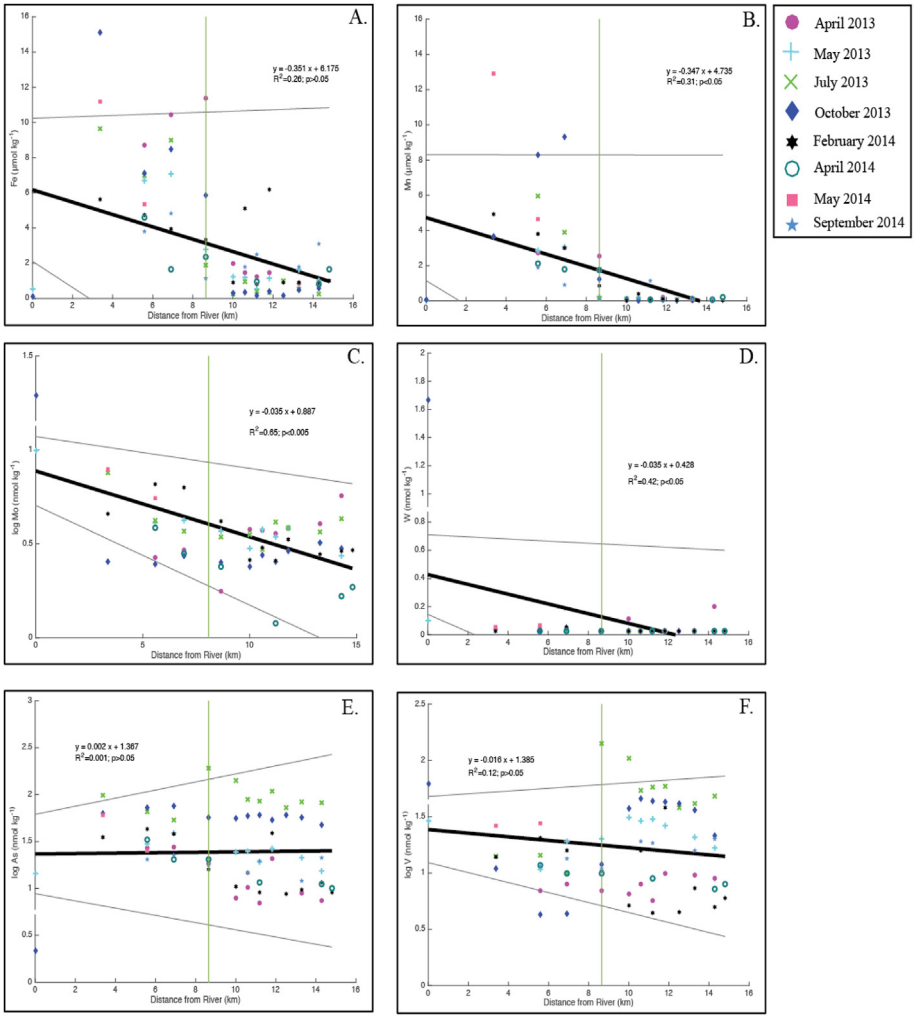

Fig. 4. Concentrations of trace elements in surface waters from the Mississippi River, Bayou Fortier, and Lac des Allemands as a function of distance from the River. The green vertical line represents the transition from Bayou Fortier to the open Lac des Allemands. A linear regression and 95% confidence intervals for the average of all sampling events at each location is also shown. Shown are dissolved Fe (A), Mn (B), Mo (C), W (D), As (E), and V (F). (For interpretation of the references to colour in this figure legend, the reader is referred to the Web version of this article.)

the sand-rich units present at EDG, VACW1, VACW2, and W4 are probably laterally continuous to the Mississippi River levee sand deposits (Kim, 2015).

Using dissolved Fe as a proxy for anoxia ($Fe \geq 100\ \mu g\ L^{-1}$ or $1.8\ \mu mol\ kg^{-1}$), all of the groundwater samples, except for the May VACW1 sample, are classified as anoxic (Wright et al., 2014; McMahon and Chapelle, 2008). Additionally, based on the classification scheme of Berner (1981), the groundwaters were both anoxic and sulfidic ($S(-II) > 1\ \mu mol\ kg^{-1}$) at all locations during the October and February sampling events (Appendix D). Together, these classifications indicate that groundwaters were generally reducing and favored the dissolution of Fe(III)/Mn(IV) oxides/oxyhydroxides, especially during the autumn and winter. Moreover, all groundwaters exhibited acidic to neutral pH, reflecting the high organic content of freshwater marsh sediments (Appendix D; Feijtel et al., 1988; Nyman et al., 1990; Neubauer et al., 2005; Swarzenski et al., 2008).

4.2. Trace element geochemistry of surface waters and groundwaters

Surface water concentrations of trace elements (Fe, Mn, Mo, W, As, and V) are presented as a function of distance from the Mississippi River (Fig. 4). Manganese and Fe concentrations are low in the Mississippi River and Lac des Allemands surface waters, but elevated concentrations of Mn and Fe are observed in Bayou Fortier surface waters (Fig. 4A and B; Appendix C). Bayou Fortier is a slow moving body of water with visible suspended matter. The dissolved Fe and Mn concentrations in Bayou Fortier surface waters are therefore likely released to surface waters from suspended sediment. In the groundwater samples, Fe and Mn concentrations are generally high ($Fe = 54.6 \pm 83.3$, $Mn = 23.2 \pm 21.7\ \mu mol\ kg^{-1}$), demonstrating the reducing conditions of the local groundwaters.

Of the trace elements, only Mo concentrations show a statistically significant variation as a function of distance from the river in surface waters from Bayou Fortier and Lac des Allemands (Fig. 4C). Vanadium and As concentrations vary between 4.31 and $140.0\ nmol\ kg^{-1}$ and 7.44–189 $nmol\ kg^{-1}$, respectively, and show no discernible trend as a function of distance (Appendix C; Fig. 4E and F). The surface water samples with exceptionally high concentrations of V and As (e.g., S3 and S5 in July) that occur seemingly randomly throughout time and location may arise from resuspension of bottom sediments within the lake. Conversely, W concentrations in the surface waters from Bayou Fortier and Lac des Allemands are low, with 90% of the sample concentrations below the detection limit (39 pmol/kg; Fig. 4D).

In contrast to the surface waters, trace element concentrations (Mo, W, As, V) of the groundwater samples vary through time and with location (Fig. 5). Two trends in the data are particularly notable. First, trace element concentrations are generally greatest in groundwaters extracted from coarse-grained sediment units. The average Mo, W, and As concentrations are 12, 2, and 10 times greater in the groundwaters from coarse-grained sediments as compared to the fine-grained sediments (Fig. 5; Appendix D). The average V concentrations, however, are not substantially different between locations with different grain-sized sediments. Second, trace element concentrations are generally elevated in October and February as compared to April, May, and September.

The computed speciation of the trace metals is shown in Fig. 6A and Appendix E. During times of elevated sulfide concentrations (i.e., October, February), thiomolybdates are predicted to form, whereas the molybdate oxyanion dominates during the spring and early fall when dissolved sulfide is substantially lower. Conversely, thioarsenate formation is predicted to occur during all seasons, although in much greater percentages in the winter and late fall.

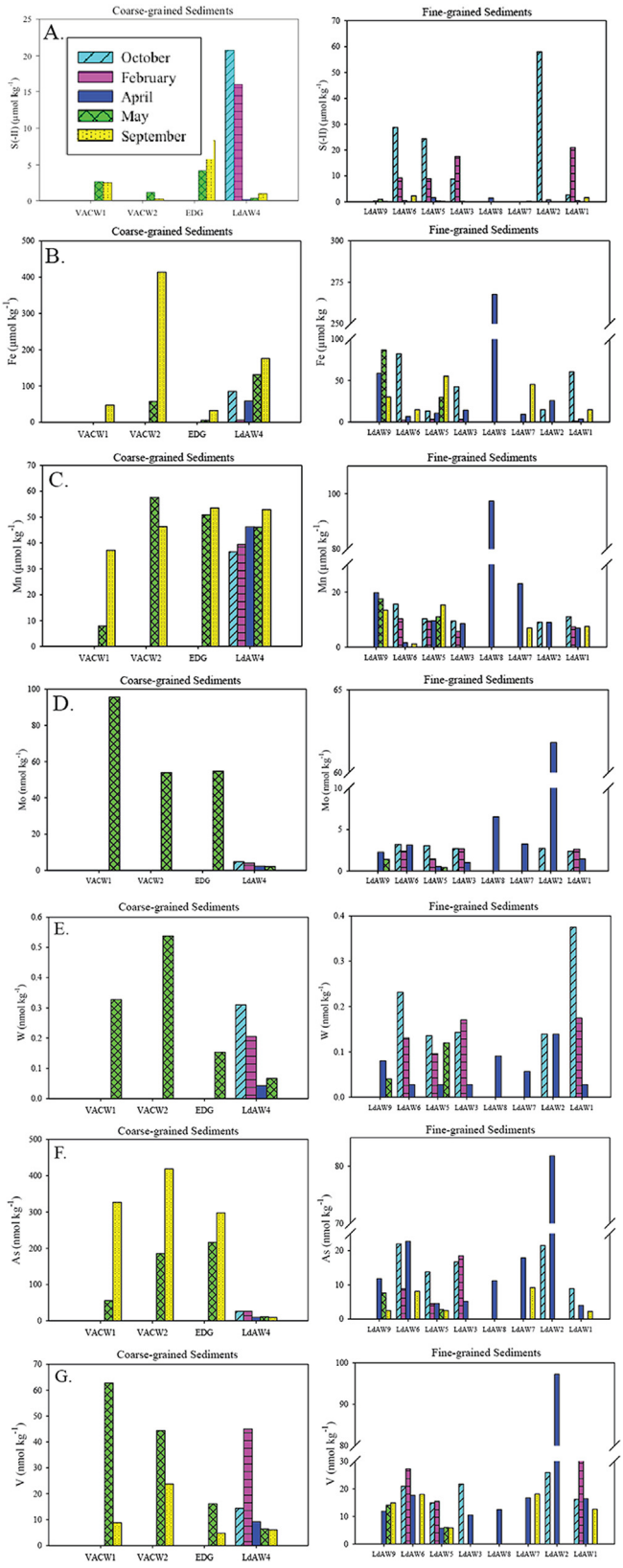

Fig. 5. Dissolved S(-II) and trace element concentrations of groundwaters from Lac des Allemands separated by samples from coarse-grained, low organic content sediments and samples from fine-grained, organic-rich sediments. Shown are (A) S(-II), (B) Fe, (C) Mn, (D) Mo, (E) W, (F) As, (G) V. Two outliers (W2, W8) from the April sampling event are excluded from further analysis.

Thiotungstate formation is not predicted to be an important process during any season. The predicted speciation is consistent with measurements of thiotungstate formation constants, which indicate that W is less reactive towards S(-II) than Mo (Mohajerin et al., 2014, 2016). Formation of thiovanadates has not been reported in natural waters (Steudel, 1996), and the speciation of V is dominated by the vanadyl cation (VO^{2+}).

Geochemical modeling also predicts that Fe–S minerals are likely to form during all seasons, especially during the late fall and winter (Fig. 6B). More specifically, mackinawite is near or below saturation, whereas pyrite is consistently oversaturated. Formation of As–S minerals is expected to be negligible.

5. Discussion

5.1. Redox conditions in the marsh

Lac des Allemands experiences negligible tidal activity, and the marsh is perpetually saturated, prohibiting aerobic conditions and hence, oxidation of deep pore waters and sediments. Thus, it is not surprising that the marsh experienced reducing conditions during all sampling events of this study. Dissolved S(-II) concentrations are not expected to be particularly high in freshwater marshes as compared to brackish and saline marshes, owing to a greater distance from an oceanic SO_4^{2-} source compared to salt marshes (DeLaune et al., 2002a; Neubauer et al., 2005). For example, gaseous H_2S emissions from freshwater marshes in Louisiana are 12 and 27 times lower than emissions from brackish and salt marshes, respectively (DeLaune et al., 2002a,b). Instead, in freshwater marshes, Fe(III) reduction has been shown to be the most important redox buffer in the early summer followed by methanogenesis later in the year (Neubauer et al., 2005). High dissolved Fe and Mn concentrations in local pore water supports the notion that redox is buffered by reductive dissolution of Fe(III)/Mn(IV) oxides/oxyhydroxides throughout the year in Lac des Allemands groundwaters. However, occasional high dissolved S(-II) concentrations in Lac des Allemands groundwaters also insinuate a seasonal S cycle. Groundwater S(-II) concentrations are high in October and February and decrease substantially by April and May. Low dissolved S(-II) concentrations continue into September, when dissolved SO_4^{2-} concentrations increase (Appendix D). Dissolved S(-II), in turn, affects the dissolved Fe(II) concentrations either by reducing Fe(III) oxides/oxyhydroxides and/or precipitating with Fe to form iron sulfide mineral phases (Dos Santos Afonso and Stumm, 1992; Kostka and Luther, 1995). Geochemical modeling indicates that pyrite is likely an important sink for Fe in this system (Fig. 6B; Appendix F).

5.2. Input from Mississippi River

Previous studies suggest that Bayou Fortier is hydrologically connected to the Mississippi River via a buried; sand-rich crevasse splay deposit that truncates near the W4 well (Figs. 1 and 2; Breaux, 2015; Kim, 2015). For example, Kim (2015) used radon as a tracer to estimate that between 0.4 and 14.6 cm day^{-1} ($2.2 \cdot 10^4$ m^3 day^{-1}) of Mississippi River derived groundwater is discharged at the head of Bayou Fortier. The surface water concentrations of dissolved trace elements observed on a transect from the Mississippi River to Lac des Allemands, suggest that the Mississippi River has the potential to supply Lac des Allemands with dissolved V, Mo and W, whereas the As concentration in the river is less than that observed in the lake, indicating that the Mississippi River is not a source of As to Lac des Allemands (Fig. 4). Tungsten, and to a greater extent, Mo, decrease significantly with distance from the river, decreasing from 1.67 nmol kg^{-1} to below detection and 19.6 to 2.46 nmol kg^{-1}, respectively, between the river and station 7 during the October sampling (Appendix C). Vanadium similarly decreases with distance from the river, but variability in the open lake concentrations obscures a definitive trend (Fig. 4). The magnitude of hydraulic head difference driving groundwater flow from the Mississippi River to the interdistributary basin varies as a function of river stage, suggesting that any transport of trace elements from the river to the lake is likely to vary seasonally (Kolker et al., 2013). Additionally, the concentrations of trace elements increased in the river between the May and October sampling trips, whereas the river stage decreased over this time, suggesting that trace element concentrations in the Mississippi River are not directly related to discharge (Fig. 4; Appendix C). For example, previous work in the Mississippi River showed that Fe and Mn are highest in the fall and decrease in the spring, whereas V and Mo display the opposite trend (Shiller, 1997). The variability in the concentration of these trace elements in Mississippi River water reflects redox processes in the river basin rather than hydrologic factors (Shiller, 1997). Better temporal resolution of the trace element concentrations in the Mississippi River as well as a hydrological constraint on the amount of water entering Lac des Allemands from Bayou des Allemands are necessary to estimate the trace element flux from surface reservoirs. However, trace element concentrations in the groundwaters at Lac des Allemands fluctuate independently of surface water variability, suggesting that in situ conditions in the deep marsh sediments overwhelm the signal from changes in surface water supply (Figs. 4 and 5). The correspondence of increased dissolved trace metal concentration with dissolved sulfide suggests that trace metals are released from the sediment under reducing conditions in the late fall and winter.

5.3. Redox-sensitive trace elements

5.3.1. Molybdenum

Previous work has demonstrated that Mo solubility decreases under reducing conditions owing to formation of thiomolybdates and subsequent sequestration as Fe–Mo–S solids. Erickson and Helz (2000) describe a geochemical switch at dissolved S(-II) concentrations greater than 11 μmol kg^{-1}, where the molybdate oxyanion, MoO_4^{2-}, is converted to thiomolybdate complexes by reaction with H_2S. More recent investigations point out that thiomolybdate anions are more particle reactive than the molybdate oxyanion, which ultimately leads to Mo removal from solution (Erickson and Helz, 2000; Vorlicek et al., 2004; Helz et al., 2014). A mechanism proposed by Vorlicek et al. (2004) attributes formation of Mo–Fe–S cuboidal clusters on pyrite formed by ligand-induced reduction of Mo(VI) by polysulfides.

However, Mo in Lac des Allemands groundwaters exhibits the opposite behavior: Mo is liberated under reducing conditions. Although the geochemical modeling predicts formation of thiomolybdates, sustained dissolved S(-II) concentrations greater than 11 μmol kg^{-1} are required for formation and persistence of thiomolybdates and sequestration of excess Mo by sediments (Erickson and Helz, 2000; Adelson et al., 2001). Thus, at the seasonal scale, Mo speciation is kinetically controlled, and Mo may still exist as molybdate in Lac des Allemands groundwaters (Erickson and Helz, 2000). Another possibility for this anamolous behavior is the influence of Fe. Low dissolved Fe concentrations favor the formation of organic S (Zaback and Pratt, 1992; Mongenot et al., 2000; Tribovillard et al., 2004), and a study of S speciation in Louisiana freshwater marsh soils indicates that organic sulfur as ester-sulfate or carbon-bonded sulfur accounts for greater than 70% of the total sulfur in local marsh soils, with minor contributions from mackinawite and pyrite (Krairapanond et al., 1992). Hence, Mo may also be associated with organic matter via bonding with S-compounds

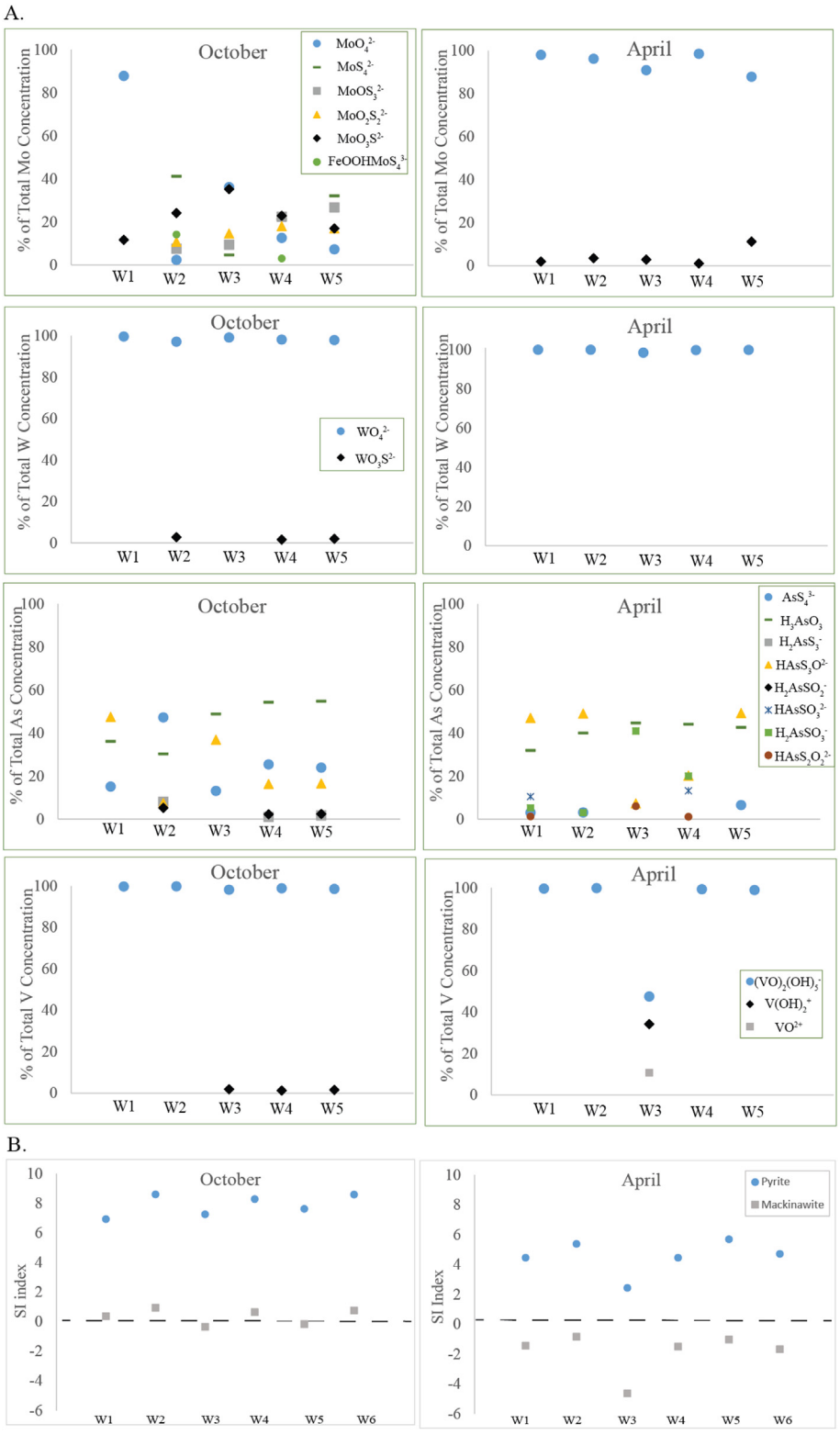

Fig. 6. A. Trace element speciation shown as percent of total element concentration. Data for additional months and wells in Appendix E. B. Saturation Indices (log Q/K) for pyrite and mackinawite. Data for additional months and wells in Appendix F.

(Helz et al., 1996; Tribovillard et al., 2004; Algeo and Lyons, 2006). Finally, reductive dissolution of Fe(III)/Mn(IV) oxides/oxy-hydroxides may have occurred and released adsorbing ions such as molybdate (Froelich et al., 1979). For example, during October and February, Mo is positively correlated with Mn ($R^2 = 0.46$; $p < 0.0005$), an association commonly recruited to explain Mo behavior (e.g., Bertine and Turekian, 1973; Crusius et al., 1996; Tribovillard et al., 2006). It is unlikely that such unexepected Mo

behavior is unique to Lac des Allemands groundwaters, and further study of Mo in seasonally variabe redox settings will help elucidate these observations.

5.3.2. Tungsten

Similar to Mo, W also exhibits higher concentrations in Lac des Allemands groundwaters in the autumn and winter than in the spring and summer (Fig. 5E; *t*-test, $p < 0.05$). Tungsten also significantly correlates with Fe in the fall/winter ($R^2 = 0.53$, $p < 0.05$), a relationship that is not observed in the spring. Given that the pH does not change appreciably between seasons, the elevated W concentrations in the fall and winter likely result from dissolution of Fe(III) oxides/oxyhydroxides rather than desorption reactions.

The molal Mo/W ratio of Lac des Allemands groundwaters (72.3 ± 113) is less than that in the surface waters (111 ± 31.9) (Mann-Whitney test, 5% significance level), which is consistent with observations of greater W enrichment in pore waters relative to surface waters in other Mississippi Delta pore waters (Mohajerin et al., 2016). Tungsten adsorption onto ferromanganese oxides is typically greater than Mo adsorption owing to the octahedral coordination and inner sphere complexation of W onto these metal oxides/oxyhydroxides as opposed to the tetrahedral coordination and outer sphere complexation of Mo adsorption (Kashiwabara et al., 2010, 2013; Gustafsson, 2003).

Arnórsson and Óskarsson (2007) also observed elevated Mo/W ratios in peat soil groundwaters, which they attributed to adsorption of W onto organic matter, clay minerals and/or Fe(III) hydroxide. Furthermore, in organic-rich sediments, adsorption onto organic matter and clays may be more important than Fe(III)/Mn(IV) oxide/oxyhydroxide surfaces (Arnórsson and Óskarsson, 2007). Tungsten adsorption experiments also indicate that W adsorption is strongest on soils with the highest organic content, but the interaction with humic substances is not detailed (Koutsospyros et al., 2006). The relationship between W and organic matter warrants further study.

Although W concentrations in the groundwaters show a seasonal trend, W concentrations in the surface waters do not vary substantially through space or time, and surface water concentrations are mostly below detection (Fig. 4D). Therefore, although W is released from the sediments into the groundwaters, most of the generated W is probably readsorbed onto marsh sediment near the sediment-water interface. The W concentrations at the bayou surface sites (S6 and S7) in October and February are detectable in contrast to the other surface water sites, which may suggest that marsh sediments release some W to the bayou, which is then scavenged by bayou bottom sediments.

5.3.3. Arsenic

Similar to the other trace elements, As concentrations in groundwaters from Lac des Allemands are higher in the fall and winter than in the spring and late summer, coincident with high dissolved S(-II) concentrations. In sulfidic waters, As(V) is predicted to form thioarsenate species (Fig. 6A). As thioarsenate, arsenic is less likely to be sequestered in the sediments (Van der Weijden et al., 1990; Kirk et al., 2010; Burton et al., 2013). Furthermore, groundwater dissolved As concentrations may be higher in the fall and winter compared to the spring because thioarsenite and thioarsenate sorb more strongly to Fe oxides/oxyhydroxides than to pyrite, and the groundwaters are more saturated with respect to pyrite during the fall and winter (Couture et al., 2013).

Nevertheless, groundwater As concentrations are less than those observed in the bayou surface waters, signifying that the deep marsh groundwaters likely serve as a sink for dissolved As. Previous studies argue that As is generally removed from waters where sulfate reduction is occurring via precipitation of arsenic-sulfide minerals or co-precipitation with iron sulfide minerals (Kirk et al., 2004, 2010; Bostick et al., 2004; Wolthers et al., 2005). Geochemical modeling indicates that these groundwaters are all undersaturated with respect to As–S species (e.g., realgar, orpiment) during all sampling events. Precipitation of arsenic sulfide species is favored under conditions of low pH (pH = 4–6), elevated As concentrations, and dissolved S(-II) concentrations low enough to prevent formation of thioarsenates/thioarsenites (Wilkin and Ford, 2006; Kirk et al., 2010). Groundwaters from Lac des Allemands generally have a circumneutral pH (5.3–8.2) and low dissolved As concentrations (55.0 ± 103 nmol kg^{-1}), indicating that precipitation of arsenic-sulfide species is not an important sink for As. Of the iron sulfide mineral phases, mackinawite is typically the first to precipitate (Schoonen and Barnes, 1991; Wolthers et al., 2005). Yet, the Lac des Allemands groundwaters are undersaturated with respect to mackinawite but are oversaturated with respect to pyrite (Appendix F). Furthermore, laboratory experiments indicate that As co-precipitation with iron sulfides occurs predominantly with pyrite (Kirk et al., 2010). Therefore, the measured dissolved As concentrations and geochemical modeling of mineral saturation states of Lac des Allemands waters are consistent with sequestration of As in pyrite.

5.3.4. Vanadium

During October and February, the groundwaters at Lac des Allemands exhibited relatively high V concentrations compared to the concentrations in the surface waters from Bayou Fortier. Conversely, the April, May, and September sampling reveal similar concentrations between the groundwaters and surface waters or, in some cases, higher V concentrations in the surface waters than the groundwaters (Figs. 4F and 5G). Therefore, during the fall and winter, the groundwaters appear to serve as a source of V to the bayou. However, because the groundwaters are relatively more reducing during the fall and winter, V is predicted to exist as vanadyl and should be less soluble due to its greater affinity for particle surfaces under reducing conditions (Fig. 6A; Breit and Wanty, 1991). Vanadium is known to sorb to Fe(III)/Mn(IV) oxides/oxyhydroxides, organic matter, and clays (McBride, 1979; Wehrli and Stumm, 1989). Yet, if the potential host phases adsorbing V dissolve, V concentrations would increase in the groundwaters. As discussed above, Fe(III)/Mn(IV) oxides/oxyhydroxides are likely undergoing reductive dissolution in deep marsh sediments in the study region. However, V does not covary with dissolved Fe concentrations ($R^2 = -0.16$, $p > 0.05$), indicating that upon reductive dissolution, Fe and V concentrations are regulated by separate mechanisms. Whereas dissolved Fe precipitates with dissolved sulfide to form iron sulfide minerals, dissolved V may be stabilized in solution by complexation with organic matter (Breit and Wanty, 1991; Wanty and Goldhaber, 1992; Lu et al., 1998; Pourret et al., 2012).

6. Summary and implications for redox sensitive trace element cycling in the Mississippi River Delta

Analysis of redox-sensitive trace elements indicates that reductive dissolution of Fe(III)/Mn(IV) oxides/oxyhydroxides during the reducing conditions of the fall and late winter are important processes for supplying trace elements to pore waters. Therefore the source of trace elements may be related to the supply of reducible Fe/Mn oxides/oxyhydroxide minerals of coatings on sediment grains. Dissolved Mn concentrations increase with

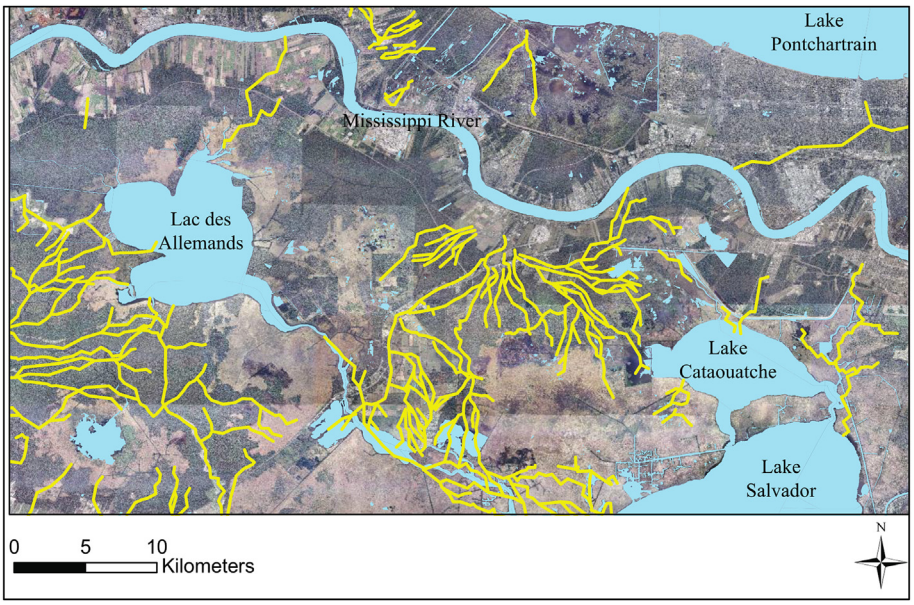

Fig. 7. Distribution of abandoned distributaries in the upper Barataria Basin (yellow). Channels were traced using Mississippi River Deltaic Plain 15-min quadrangle maps from the U.S. Army Corps and overlain on a compilation of high resolution orthoimagery from the USGS EarthExplorer database. (For interpretation of the references to colour in this figure legend, the reader is referred to the Web version of this article.)

increasing grain size of the surrounding sediment, which explains why the farmland wells and Lac des Allemands well W4 have relatively high dissolved Mn concentrations and commonly exhibit higher trace element concentrations. This relationship is not observed for dissolved Fe concentrations, but Fe is reprecipitated as sulfide mineral as dissolved S(-II) concentrations increase. These results suggest that buried sand units with Fe(III)/Mn(IV) oxide/oxyhydroxide coatings throughout the delta may serve as sources of dissolved trace element to pore waters and possibly surface waters, but more work to quantify the association of trace elements in the solid phase is necessary to determine the exact source of the trace elements. Fig. 7 shows a distribution of sand units throughout the Lac des Allemands region, which indicates numerous abandoned distributary channels that extend to the natural levee deposit of the Mississippi River. Where the distributary channels are connected to interdistributary lakes and bayous, they may serve as a source of trace elements to the basin and ultimately the Gulf of Mexico.

The marsh pore waters are also tightly coupled to redox reactions, including not only Fe(III) and Mn(IV) reduction but also sulfate reduction. In particular, trace element concentrations (Mo, W, As, V) increase in October and February, coinciding with more reducing conditions in marsh groundwaters. The increase in concentration is expected for W and As and is most pronounced for W. The increase in Mo and V concentrations, however, requires further explanation as both elements are expected to be more particle reactive under reducing conditions. The unexpected solubility of V has been demonstrated in other reducing basins, such as Framvarren Fjord and is attributed to aqueous complexation with dissolved organic carbon (Emerson and Huested, 1991). Such a mechanism is likely also operating in the organic-rich waters at Lac des Allemands. The cause of Mo solubility under reducing conditions is less certain as most studies in reducing basins report sequestration of Mo even with sporadic H_2S (e.g., Tribovillard et al., 2006). Molybdenum's persistence in reducing waters is likely related to kinetic effects. If so, this study suggests that in pore waters with seasonally variable redox conditions, Mo sequestration may not record paleoredox conditions as well as previously thought.

The marsh surrounding Lac des Allemands is typical of freshwater marsh systems and demonstrates that local groundwaters are rich in organic matter and electron acceptors that actively drive redox reactions. These reactions, in turn, affect trace element sequestration in sediments and potential supply to the interdistributary basin. This study also underscores the need for a better understanding of organic matter interaction with trace elements that form aqueous complexes with sulfur.

Acknowledgements

We would like to thank Cyndhia Ramatchandirane, Minming Cui, Michael Freeman, and Jill Arriola for assistance with field work, Airboat Arthur's for dock use and mechanical assistance, Dr. Deborah Grimm for assistance with ICP-MS analysis, and Dr. Christopher White for expertise with statistical analysis. We would also like to thank Mike Falgoust and the farming communities of Vacherie, LA and Edgard, LA that let us install wells. We would also like to thank Dr. Trent Vorlicek and an anonymous reviewer as well as AE Dr. Stephen Skrabal, whose comments greatly improved this manuscript. This work was funded by a National Science Foundation grant (NSF EAR-1141692) to K. H. Johannesson, NSF grant EAR-1141716 to A. S. Kolker, and NSF grant EAR-1141685 to J. E. Cable through the Hydrological Sciences program and the Vokes Fellowship from Tulane University.

Appendix A. Sample identification and location for surface water and groundwater sites

Sample Name	Latitude	Longitude	Location Type	Well Depths (cm below surface)	Dates Sampled
Mississippi River (MSR)	29.9383	−90.3547	Surface Water	NA	2013: May, Oct.
LdA-S0	29.8809	−90.5278	Surface Water	NA	2014: Feb., April
LdA-S1	29.8875	−90.5392	Surface Water	NA	2013: April, May, July, Oct. 2014: Feb, April, Sept.
LdA-S2	29.9260	−90.5525	Surface Water	NA	2013: April, May, July, Oct. 2014: Feb, April, Sept.
LdA-S3	29.9520	−90.5612	Surface Water	NA	2013: April, May, July, Oct. 2014: Feb.
LdA-S5	29.9701	−90.5628	Surface Water	NA	2013: April, May, July, Oct. 2014: Feb, April, Sept.
LdA-S6	29.9837	−90.5529	Surface Water	NA	2013: April, May, July, Oct. 2014: Feb, April, Sept.
LdA-S7	29.9944	−90.5441	Surface Water	NA	2013: April, May, July, Oct. 2014: Feb., April, May, Sept.
LdA-S8	29.9372	−90.6251	Surface Water	NA	2013: April, May, July, Oct. 2014: Feb., Sept.
LdA-S9	29.9244	−90.6231	Surface Water	NA	2013: April, May, July, Oct. 2014: Feb.
LdA-S10	29.9111	−90.5948	Surface Water	NA	2013: April, May, July, Oct. 2014: Feb., Sept.
LdA-S11	29.9210	−90.5852	Surface Water	NA	2013: July, Oct. 2014: Feb.
St-8	30.0139	−90.5431	Surface Water	NA	2013: July, Oct. 2014: Feb., May
LdA-W1	29.9743	−90.5581	Marsh	200	2013: Oct. 2014: Feb., April, Sept.
LdA-W2	29.9747	−90.5582	Marsh	108	2013: Oct. 2014: April
LdA-W3	29.9822	−90.5533	Marsh	55	2013: Oct. 2014: Feb., April
LdA-W4	29.9945	−90.5444	Marsh	175	2013: Oct. 2014: Feb., April, May
LdA-W5	29.9878	−90.5528	Marsh	280	2013: Oct. 2014: Feb., April, May
LdA-W6	29.9880	−90.5531	Marsh	345	2013: Oct. 2014: Feb., April
LdA-W7	29.9770	−90.5584	Marsh	196	2014: April, Sept.
LdA-W8	29.9770	−90.5583	Marsh	235	2014: April
LdA-W9	29.9885	−90.5535	Marsh	254	2014: April, May, Sept.
EDG	30.0461	−90.5714	Farmland	875	2014: May, Sept.
VAC-1	29.9356	−90.6667	Farmland	183	2014: May, Sept.
VAC-2	29.9356	−90.6667	Farmland	488	2014: May, Sept.

Appendix B. Detection limits were calculated as three times the standard deviation of the blank, where the standard deviation was calculated from the blank concentrations of each element for all ICP-MS analyses

	Detection Limits	Reported as DL/$\sqrt{2}$
Mo	82 pmol/kg	58 pmol/kg
W	39 pmol/kg	28 pmol/kg
U	22 pmol/kg	16 pmol/kg
V	175 pmol/kg	124 pmol/kg
Mn	917 pmol/kg	648 pmol/kg
Fe	31 nmol kg^{-1}	22 pmol/kg
Al	10 nmol kg^{-1}	7 pmol/kg
As	674 pmol/kg	477 pmol/kg

Appendix C. Temperature, pH, conductivity, salinity, major solute, and trace element concentrations in surface waters from Lac des Allemands, Bayou Fortier, and the Mississippi River

		MSR	LdA-S0	LdA-S1	LdA-S2	LdA-S3	LdA-S5	LdA-S6
Temperature (°C)	Apr-13	ND	ND	23.40	22.70	22.00	25.90	24.50
	May-13	ND	ND	26.23	27.16	28.26	29.24	28.48
	Jul-13	ND	ND	30.94	30.57	30.53	32.48	32.2
	Oct-13	ND	ND	28.00	28.30	29.10	28.30	29.50
	Feb-14	ND	18.90	19.60	20.10	18.90	19.20	19.20
	Apr-14	ND	18.37	18.02	18.12	ND	17.65	17.04
	May-14	ND	ND	ND	ND	ND	ND	ND
	Sep-14	ND	ND	26.30	26.72	ND	27.46	27.21
Conductivity (μS cm^{-1})								
	Apr-13	ND	ND	ND	ND	ND	ND	ND
	May-13	ND	ND	0.125	0.16	0.159	0.139	0.154
	Jul-13	ND	ND	0.145	0.141	0.153	0.166	0.224
	Oct-13	ND	ND	ND	ND	ND	188	185
	Feb-14	ND	180	160	172	164	233	234
	Apr-14	ND	183	174	176	ND	186	200
	May-14	ND	ND	ND	ND	ND	ND	ND
	Sep-14	ND	ND	153	148	ND	153	160
Salinity (psu)								
	Apr-13	ND	ND	0.07	0.07	0.07	0.07	0.07
	May-13	ND	ND	0.06	0.07	0.07	0.06	0.07
	Jul-13	ND	ND	0.07	0.06	0.07	0.08	0.10
	Oct-13	ND	ND	0.07	0.07	0.08	0.08	0.09
	Feb-14	ND	0.10	0.08	0.09	0.09	0.12	0.13
	Apr-14	ND	0.09	0.08	0.08	ND	0.09	0.09
	May-14	ND	ND	ND	ND	ND	ND	ND
	Sep-14	ND	ND	0.07	0.07	ND	0.07	0.07
pH								
	Apr-13	ND	ND	ND	ND	ND	ND	ND
	May-13	ND	ND	9.65	10.08	10.11	9.35	7.46
	Jul-13	ND	ND	8.94	8.64	9.23	9.13	7.74
	Oct-13	ND	ND	6.95	ND	ND	6.70	6.61
	Feb-14	ND	8.54	8.82	9.24	9.38	7.71	7.04
	Apr-14	ND	7.51	7.77	8.88	ND	ND	6.80
	May-14	ND	ND	ND	ND	ND	ND	ND
	Sep-14	ND	ND	7.60	8.37	ND	8.90	7.88
DOC (mmol L^{-1})								
	Apr-13	ND	ND	ND	ND	ND	ND	ND
	May-13	ND	ND	ND	ND	ND	ND	ND
	Jul-13	ND	ND	ND	ND	ND	ND	ND
	Oct-13	ND	ND	0.874	0.874	0.768	1.16	1.19
	Feb-14	ND	0.795	0.570	0.720	1.02	0.501	1.05
	Apr-14	ND	2.01	1.87	1.90	ND	2.19	2.35
	May-14	ND	ND	ND	ND	ND	ND	ND
	Sep-14	ND	ND	0.967	0.796	ND	0.773	0.742
TN (μmol L^{-1})								
	Apr-13	ND	ND	ND	ND	ND	ND	ND
	May-13	ND	ND	ND	ND	ND	ND	ND
	Jul-13	ND	ND	ND	ND	ND	ND	ND
	Oct-13	ND	ND	49.3	48.4	49.1	52.8	53.1
	Feb-14	ND	50.3	49.4	43.4	49.8	38.9	30.4
	Apr-14	ND	60.8	49.9	51.8	ND	54.7	45.9
	May-14	ND	ND	ND	ND	ND	ND	ND
	Sep-14	ND	ND	54.6	44.9	ND	41.5	43.0
mmol kg^{-1}								
Mg								
	Apr-13	ND	ND	0.20	0.19	0.20	0.21	0.28
	May-13	0.275	ND	0.15	0.20	0.15	0.16	0.19
	Jul-13	ND	ND	0.16	0.16	0.15	0.17	0.26
	Oct-13	0.649	ND	0.223	0.214	0.215	0.247	0.280
	Feb-14	ND	0.246	0.217	0.218	0.214	0.292	0.332
	Apr-14	ND	0.213	0.189	0.208	ND	0.222	0.262
	May-14	ND	ND	ND	ND	ND	ND	ND
	Sep-14	ND	ND	0.149	0.172	ND	0.185	0.158

(*continued*)

		MSR	LdA-S0	LdA-S1	LdA-S2	LdA-S3	LdA-S5	LdA-S6
Ca								
	Apr-13	ND	ND	0.158	0.148	0.150	0.189	0.281
	May-13	0.325	ND	0.109	0.150	0.105	0.119	0.172
	Jul-13	ND	ND	0.106	0.101	0.112	0.117	0.253
	Oct-13	0.613	ND	0.142	0.150	0.153	0.202	0.250
	Feb-14	ND	0.210	0.190	0.193	0.190	0.284	0.345
	Apr-14	ND	0.267	0.248	0.302	ND	0.233	0.291
	May-14	ND	ND	ND	ND	ND	ND	ND
	Sep-14	ND	ND	0.199	0.216	ND	0.227	0.238
Na								
	Apr-13	ND	ND	0.54	0.52	0.53	0.43	0.51
	May-13	0.434	ND	0.40	0.58	0.44	0.40	0.38
	Jul-13	ND	ND	0.45	0.45	0.46	0.48	0.56
	Oct-13	1.62	ND	0.637	0.541	0.546	0.615	0.550
	Feb-14	ND	1.04	0.829	0.794	0.803	0.803	0.726
	Apr-14	ND	1.25	0.756	1.00	ND	0.721	0.659
	May-14	ND	ND	ND	ND	ND	ND	ND
	Sep-14	ND	ND	0.378	0.458	ND	0.509	0.472
$^{*}SO_4^{2-}$								
	Apr-13	ND	ND	ND	ND	ND	ND	ND
	May-13	ND	ND	0.125	0.021	**0.014**	0.021	**0.014**
	Jul-13	ND	ND	ND	ND	ND	ND	ND
	Oct-13	ND	ND	**0.014**	**0.014**	**0.014**	**0.014**	**0.014**
	Feb-14	ND	**0.014**	**0.014**	**0.014**	**0.014**	**0.014**	**0.014**
	Apr-14	ND	**0.014**	**0.014**	ND	ND	**0.014**	**ND**
	May-14	ND	ND	ND	ND	ND	ND	ND
	Sep-14	ND	ND	1.67	1.15	ND	**0.014**	**0.014**
Alkalinity (as HCO_3^-)								
	Apr-13	ND	ND	ND	ND	ND	ND	ND
	May-13	ND	ND	ND	ND	ND	ND	ND
	Jul-13	ND	ND	ND	ND	ND	ND	ND
	Oct-13	ND	ND	6.79	8.23	9.75	10.5	11.2
	Feb-14	ND	0.880	0.896	0.688	0.872	1.18	1.50
	Apr-14	ND	1.60	1.04	0.960	ND	0.960	1.12
	May-14	ND	ND	ND	ND	ND	ND	ND
	Sep-14	ND	ND	0.510	ND	ND	0.680	1.27
$\mu mol\ kg^{-1}$								
K								
	Apr-13	ND	ND	50.26	46.09	47.32	33.72	36.18
	May-13	45.9	ND	42.14	56.76	43.19	38.29	37.94
	Jul-13	ND	ND	49.63	46.83	45.73	43.49	51.59
	Oct-13	97.5	ND	51.2	47.2	49.8	61.0	66.3
	Feb-14	ND	73.4	64.3	65.7	62.5	81.8	82.7
	Apr-14	ND	182	57.3 ± 5.40	144	ND	55.3	73.2
	May-14	ND	ND	ND	ND	ND	ND	ND
	Sep-14	ND	ND	76.9	74.5	ND	73.9	70.5
Ba								
	Apr-13	ND	ND	ND	ND	ND	ND	ND
	May-13	ND	ND	0.23	0.27	0.27	0.23	0.25
	Jul-13	ND	ND	ND	ND	ND	ND	ND
	Oct-13	0.576	ND	0.310	0.355	0.367	0.374	0.302
	Feb-14	ND	ND	ND	ND	ND	ND	ND
	Apr-14	ND	.966 ± 0.403	0.374 ± 0.087	0.436	ND	0.330	0.383
	May-14	ND	ND	ND	ND	ND	ND	ND
	Sep-14	ND	ND	0.392	2.58	ND	0.350	0.398
Sr								
	Apr-13	ND	ND	0.57	0.55	0.56	0.58	0.81
	May-13	0.873	ND	0.40	0.55	0.38	0.38	0.54
	Jul-13	ND	ND	0.42	0.42	0.46	0.44	0.74
	Oct-13	2.60	ND	0.742	0.748	0.764	0.855	0.947
	Feb-14	ND	1.10	1.02	1.043	1.07	1.29	1.364
	Apr-14	ND	1.94 ± 0.819	0.852 ± 0.085	0.945	ND	0.759	0.954
	May-14	ND	ND	ND	ND	ND	ND	ND
	Sep-14	ND	ND	1.05	0.752	ND	0.856	0.976
Fe								
	Apr-13	ND	ND	0.72	1.23	1.98	11.38	10.43
	May-13	0.520	ND	1.00	0.53	1.24	2.78	7.10
	Jul-13	ND	ND	0.26	0.41	0.27	1.89	8.98
	Oct-13	0.124 ± .0400	ND	0.585 ± 0.078	0.145	0.284 ± 0.071	5.87	8.48
	Feb-14	ND	1.02	0.927	0.813	0.915	3.32	3.93
	Apr-14	ND	1.66	0.820	0.981	ND	2.37	1.67

(*continued on next page*)

(*continued*)

		MSR	LdA-S0	LdA-S1	LdA-S2	LdA-S3	LdA-S5	LdA-S6
	May-14	ND	ND	ND	ND	ND	ND	ND
	Sep-14	ND	ND	3.12	2.51	ND	1.13	4.85
*Fe(II)								
	Apr-13	ND	ND	0.72	0.36	ND	1.79	1.97
	May-13	0.179	ND	0.90	0.36	**0.255**	5.37	1.25
	Jul-13	ND	ND	ND	ND	ND	ND	ND
	Oct-13	ND	ND	**0.255**	0.720	0.900	0.180	2.52
	Feb-14	ND	1.43	1.25	1.07	0.716	1.25	4.12
	Apr-14	ND	4.30	**0.255**	3.04	ND	6.09	7.70
	May-14	ND	ND	ND	ND	ND	ND	ND
	Sep-14	ND	ND	**0.255**	**0.255**	ND	**0.255**	**0.255**
*Fe_{Total}								
	Apr-13	ND	ND	10.4	3.94	ND	27.8	22.2
	May-13	ND	ND	ND	ND	ND	ND	ND
	Jul-13	ND	ND	ND	ND	ND	ND	ND
	Oct-13	ND	ND	ND	ND	ND	ND	ND
	Feb-14	ND	9.85	12.4	8.77	7.52	12.2	25.1
	Apr-14	ND	10.9	11.1	9.49	ND	27.9	36.9
	May-14	ND	ND	ND	ND	ND	ND	ND
	Sep-14	ND	ND	4.83	1.07	ND	1.79	2.69
Mn								
	Apr-13	ND	ND	0.031	0.033	0.031	2.54	3.03
	May-13	0.031	ND	0.057	0.078	0.097	0.199	3.07
	Jul-13	ND	ND	0.054	0.051	0.120	0.167	3.92
	Oct-13	0.077 ± 0.008	ND	0.052 ± 0.024	0.054	0.057 ± 0.004	1.24	9.30
	Feb-14	ND	0.028 ± 0.015	0.021 ± 0.004	0.023	0.026	0.867	3.01
	Apr-14	ND	0.200	0.058 ± 0.010	0.061	ND	1.74	1.80
	May-14	ND	ND	ND	ND	ND	ND	ND
	Sep-14	ND	ND	0.112	1.16	ND	0.111	0.922
*S(-II)								
	Apr-13	ND	ND	1.53	1.28	ND	0.655	0.530
	May-13	6.55	ND	1.50	1.90	2.03	1.53	0.81
	Jul-13	ND	ND	ND	ND	ND	ND	ND
	Oct-13	ND	ND	0.811	1.22	1.37	1.22	0.312
	Feb-14	ND	2.68	2.00	2.46	2.40	1.40	3.80
	Apr-14	ND	1.56	3.21	2.99	ND	4.80	3.59
	May-14	ND	ND	ND	ND	ND	ND	ND
	Sep-14	ND	ND	**0.219**	**0.219**	ND	0.717	1.22
nmol kg^{-1}								
Mo								
	Apr-13	ND	ND	5.67	3.59	3.78	1.77	2.93
	May-13	9.9	ND	2.74	3.45	3.00	3.71	4.20
	Jul-13	ND	ND	4.29	4.11	3.55	3.44	3.70
	Oct-13	19.6	ND	2.97	2.53	2.38	2.49	2.72
	Feb-14	ND	2.94	2.91	2.56	2.60	4.18	6.28
	Apr-14	ND	1.85	1.66	1.20	ND	2.39	2.81
	May-14	ND	ND	ND	ND	ND	ND	ND
	Sep-14	ND	ND	ND	ND	ND	ND	ND
W			0.989					
	Apr-13	ND	ND	0.203	**0.028**	0.112 ± 0.245	**0.028**	**0.028**
	May-13	0.105	ND	**0.028**	**0.028**	**0.028**	**0.028**	**0.028**
	Jul-13	ND	ND	**0.028**	**0.028**	**0.028**	**0.028**	**0.028**
	Oct-13	1.674	ND	**0.028**	**0.028**	**0.028**	**0.028**	0.047
	Feb-14	ND	**0.028**	**0.028**	**0.028**	**0.028**	**0.028**	0.056
	Apr-14	ND	**0.028**	**0.028**	**0.028**	ND	**0.028**	**0.028**
	May-14	ND	ND	ND	ND	ND	ND	ND
	Sep-14	ND	ND	ND	ND	ND	ND	ND
U								
	Apr-13	ND	ND	ND	ND	ND	ND	ND
	May-13	ND	ND	ND	ND	ND	ND	ND
	Jul-13	ND	ND	ND	ND	ND	ND	ND
	Oct-13	4.11	ND	0.411 ± 0.055	0.612	0.553	0.232	0.102
	Feb-14	ND	0.636	0.688	0.605	0.663	0.611 ± 0.155	0.583
	Apr-14	ND	0.548	0.749	1.04	ND	0.289	0.431
	May-14	ND	ND	ND	ND	ND	ND	ND
	Sep-14	ND	ND	0.281	0.231	ND	0.210	0.251 ± .0462
V								
	Apr-13	ND	ND	8.89	5.74	6.50	6.95	8.01
	May-13	29.0	ND	16.5	30.4	31.2	19.8	19.1
	Jul-13	ND	ND	47.8	57.2	104	140	10.1
	Oct-13	62.0	ND	21.5	44.0	37.6	12.1	4.39
	Feb-14	ND	5.99	5.00	4.46	5.17	10.5	15.8

(*continued*)

		MSR	LdA-S0	LdA-S1	LdA-S2	LdA-S3	LdA-S5	LdA-S6
	Apr-14	ND	7.91	7.21	8.92	ND	10.1	9.95
	May-14	ND	ND	ND	ND	ND	ND	ND
	Sep-14	ND	ND	20.1	18.8	ND	10.9	13.4
Al								
	Apr-13	ND	ND	ND	ND	ND	ND	ND
	May-13	ND	ND	ND	ND	ND	ND	ND
	Jul-13	ND	ND	ND	ND	ND	ND	ND
	Oct-13	1363	ND	139	275	270	220	232
	Feb-14	ND	2242	2612	2494	2827	1245	1079
	Apr-14	ND	2513	1107	1173	ND	320	160
	May-14	ND	ND	ND	ND	ND	ND	ND
	Sep-14	ND						
As								
	Apr-13	ND	ND	7.44	7.02 ± 1.07	7.91	18.7	27.6
	May-13	14.6	ND	15.3	19.1	24.6	20.3	39.3
	Jul-13	ND	ND	82.0	85.7	140	189	54.0
	Oct-13	2.19	ND	47.8	60.7	56.3	57.0	75.3
	Feb-14	ND	9.05	11.5 ± 4.03	9.01	10.4	16.0	38.3
	Apr-14	ND	9.98	11.2	11.5	ND	20.2	20.4
	May-14	ND	ND	ND	ND	ND	ND	ND
	Sep-14	ND	ND	21.4	19.4	ND	17.9	22.5
As (III)								
	Apr-13	ND	ND	0.850 ± 0.147	ND	ND	1.82	2.37
	May-13	ND	ND	ND	ND	ND	ND	ND
	Jul-13	ND	ND	ND	ND	ND	ND	ND
	Oct-13	ND	ND	1.57 ± 0.254	1.03 ± 0.200	0.933 ± 0.240	3.89	245 ± 30.1
	Feb-14	ND	1.57	1.60	2.10	1.86	2.19	8.47
	Apr-14	ND	2.41	1.78	1.97	ND	3.51	3.31
	May-14	ND	ND	ND	ND	ND	ND	ND
	Sep-14	ND	ND	2.35	3.94	ND	3.13	5.23

	LdA-S7	LdA-S8	LdA-S9	LdA-S10	LdA-S11	St-8
Temperature (°C)	24.50	ND	ND	ND	ND	ND
	27.41	28.56	28.04	27.63	ND	ND
	30.4	33.05	34.31	31.39	31.23	25.19
	26.40	31.00	31.90	31.50	29.90	ND
	19.10	ND	ND	ND	ND	12.40
	16.79	ND	ND	ND	ND	ND
	24.89	ND	ND	ND	ND	26.90
	27.41	ND	ND	ND	ND	ND
Conductivity (μS cm^{-1})						
	ND	ND	ND	ND	ND	ND
	0.144	0.151	0.141	0.116	ND	ND
	0.238	0.169	0.175	0.136	0.126	0.193
	190	ND	ND	ND	ND	ND
	239	ND	ND	ND	ND	189
	238	ND	ND	ND	ND	ND
	159	ND	ND	ND	ND	342
	167	ND	ND	ND	ND	ND
Salinity (psu)						
	0.07	ND	ND	ND	ND	ND
	0.07	0.07	0.07	0.05	ND	ND
	0.11	0.08	0.08	0.06	0.06	0.09
	0.09	0.08	0.08	0.08	0.09	ND
	0.13	ND	ND	ND	ND	0.09
	0.11	ND	ND	ND	ND	ND
	0.07	ND	ND	ND	ND	0.15
	0.07	ND	ND	ND	ND	ND
pH						
	ND	ND	ND	ND	ND	ND
	7	9.97	9.78	9.15	ND	ND
	7.67	9.27	9.46	8.03	7.92	6.81
	6.70	ND	ND	ND	ND	ND
	7.05	9.10	8.58	9.26	9.50	7.20
	6.85	ND	ND	ND	ND	ND
	6.82	ND	ND	ND	ND	7.09
	7.50	8.35	ND	8.21	ND	ND
DOC (mmol L^{-1})						
	ND	ND	ND	ND	ND	ND
	ND	ND	ND	ND	ND	ND

(*continued on next page*)

(*continued*)

	LdA-S7	LdA-S8	LdA-S9	LdA-S10	LdA-S11	St-8
	ND	ND	ND	ND	ND	ND
	1.39	0.924	0.941	0.874	0.858	ND
	0.908	0.858	0.874	1.36	0.966	ND
	2.67	ND	ND	ND	ND	ND
	1.38	ND	ND	ND	ND	1.45
	0.950	0.915	ND	0.668	ND	ND
TN (μmol L^{-1})						
	ND	ND	ND	ND	ND	ND
	ND	ND	ND	ND	ND	ND
	ND	ND	ND	ND	ND	ND
	98.3	58.6	58.1	56.3	53.4	ND
	48.6	46.2	52.0	86.3	48.5	ND
	47.9	ND	ND	ND	ND	ND
	168.4	ND	ND	ND	ND	138
	59.3	62.5	ND	43.3	ND	ND
mmol kg^{-1}						
Mg						
	0.29	0.19	0.20	0.20	ND	ND
	0.21	0.18	0.13	0.18	ND	ND
	0.29	0.18	0.18	0.17	0.17	0.30
	0.272	0.212	0.200	0.211	0.242	0.260
	0.356	0.216	0.208	0.218	0.210	0.418
	0.305	ND	ND	ND	ND	ND
	0.172	ND	ND	ND	ND	0.394
	0.200	0.159	ND	0.151	ND	ND
Ca						
	0.282	0.150	0.165	0.141	ND	ND
	0.204	0.144	0.098	0.140	ND	ND
	0.285	0.134	0.134	0.108	0.115	0.313
	0.247	0.156	0.147	0.132	0.142	0.243
	0.369	0.198	0.201	0.191	0.184	0.457
	0.330	ND	ND	ND	ND	ND
	0.244 ± 0.025	ND	ND	ND	ND	0.483
	0.270	0.227	ND	0.198	ND	ND
Na						
	0.55	0.51	0.50	0.56	ND	ND
	0.51	0.51	0.37	0.43	ND	ND
	0.61	0.48	0.48	0.42	0.42	0.47
	0.566	0.576	0.539	0.611	0.697	0.538
	0.793	0.741	0.699	0.790	0.751	0.496
	0.740	ND	ND	ND	ND	ND
	0.193	ND	ND	ND	ND	0.408 ± 0.053
	0.561	0.457	ND	0.346	ND	ND
$^{*}SO_4^{2-}$						
	ND	ND	ND	ND	ND	ND
	0.010	0.229	0.010	0.479	ND	ND
	ND	ND	ND	ND	ND	**0.014**
	0.014	**0.014**	1.000	**0.014**	**0.014**	ND
	0.014	0.312	0.073	1.312	2.040	ND
	1.000	ND	ND	ND	ND	ND
	0.094	ND	ND	ND	ND	ND
	0.014	0.562	ND	**0.014**	ND	ND
Alkalinity (as HCO_3^-)						
	ND	ND	ND	ND	ND	ND
	ND	ND	ND	ND	ND	ND
	ND	ND	ND	ND	ND	ND
	20.1	10.0	10.7	8.15	9.51	ND
	1.55	0.576	0.808	0.936	0.816	1.72
	1.60	ND	ND	ND	ND	ND
	0.160	ND	ND	ND	ND	0.640
	0.510	0.510	ND	2.12	ND	ND
μmol kg^{-1}						
K						
	34.55	43.80	43.30	49.52	ND	ND
	40.93	52.89	37.97	53.85	ND	ND
	59.55	46.78	48.19	49.04	51.70	109.54
	70.5	51.6	50.1	51.7	52.0	66.2
	83.7	68.6	73.0	65.9	64.3	72.2
	0.0	ND	ND	ND	ND	ND
	60.8	ND	ND	ND	ND	85.8
	66.9	72.6	ND	66.2	ND	ND

(*continued*)

	LdA-S7	LdA-S8	LdA-S9	LdA-S10	LdA-S11	St-8
Ba						
	ND	ND	ND	ND	ND	ND
	0.23	0.18	0.18	0.18	ND	ND
	ND	ND	ND	ND	ND	ND
	0.287	0.335	0.303	0.304	0.336	0.355
	ND	ND	ND	ND	ND	ND
	0.374	ND	ND	ND	ND	ND
	0.414	ND	ND	ND	ND	0.510
	0.413	0.345	ND	0.323	ND	ND
Sr						
	0.82	0.53	0.52	0.53	ND	ND
	0.67	0.52	0.35	0.51	ND	ND
	0.79	0.49	0.44	0.45	0.45	0.89
	0.928	0.758	0.727	0.712	0.782	0.907
	1.47	0.982	1.03	0.979	0.976	1.60
	1.10	ND	ND	ND	ND	ND
	ND	ND	ND	ND	ND	ND
	0.880	0.901	ND	0.781	ND	ND
Fe						
	8.71	1.49	1.48	0.87	ND	ND
	6.70	1.18	1.16	1.65	ND	ND
	6.98	0.94	0.34	0.56	1.01	9.67
	7.11	0.340	0.390	0.512	0.175	15.1
	4.76	5.13	6.18	0.891	0.922	5.64
	4.59	ND	ND	ND	ND	ND
	5.36	ND	ND	ND	ND	11.2
	3.80	1.78	ND	1.81	ND	ND
*Fe(II)						
	1.61	1.25	1.07	0.36	ND	ND
	0.90	**0.255**	**0.255**	0.36	ND	ND
	ND	ND	ND	ND	ND	2.86
	2.16	0.180	**0.255**	0.180	0.360	ND
	4.83	1.07	1.97	ND	ND	3.22
	3.76	ND	ND	ND	ND	ND
	5.73	ND	ND	ND	ND	ND
	0.255	**0.255**	ND	**0.255**	ND	ND
*Fe_{Total}						
	20.2	10.4	9.13	7.16	ND	ND
	ND	ND	ND	ND	ND	ND
	ND	ND	ND	ND	ND	ND
	ND	ND	ND	ND	ND	ND
	24.2	12.7	17.0	ND	ND	33.1
	6.27	ND	ND	ND	ND	ND
	29.0	ND	ND	ND	ND	ND
	19.9	7.70	ND	3.40	ND	ND
Mn						
	2.72	0.023	0.187	0.030	ND	ND
	2.89	0.110	0.105	0.139	ND	ND
	5.96	0.113	0.070	0.134	0.088	16.20
	8.29	0.046	0.093	0.115	0.036	3.69
	3.81	0.413	0.096	0.024	0.025	4.93
	2.13	ND	ND	ND	ND	ND
	4.64	ND	ND	ND	ND	12.9
	1.87	0.153	ND	0.088	ND	ND
*S(-II)						
	0.312	2.15	1.22	2.50	ND	ND
	0.50	1.59	1.06	1.43	ND	ND
	ND	ND	ND	ND	ND	1.25
	0.312	1.15	1.34	1.19	1.25	ND
	2.49	2.90	8.33	3.18	2.31	1.37
	3.03	ND	ND	ND	ND	ND
	5.36	ND	ND	ND	ND	ND
	0.967	0.998	ND	1.40	ND	ND
nmol kg^{-1}						
Mo						
	2.67	3.72	3.80	4.05	ND	ND
	4.07	3.75	3.83	3.19	ND	ND
	4.20	2.94	3.85	3.67	3.35	7.51

(*continued on next page*)

(*continued*)

	LdA-S7	LdA-S8	LdA-S9	LdA-S10	LdA-S11	St-8
	2.46	2.76	2.90	3.22	3.37	2.53
	6.57	3.02	3.33	2.79	2.30	4.57
	3.84	ND	ND	ND	ND	ND
	5.51	ND	ND	ND	ND	7.88
	ND	ND	ND	ND	ND	ND
W						
	0.028	**0.028**	**0.028**	**0.028**	ND	ND
	0.028	**0.028**	**0.028**	**0.028**	ND	ND
	0.028	**0.028**	**0.028**	**0.028**	ND	ND
	0.028	**0.028**	**0.028**	**0.028**	**0.028**	0.040 ± 0.005
	0.049	**0.028**	**0.028**	**0.028**	**0.028**	**0.028**
	0.028	ND	ND	ND	ND	ND
	0.066 ± 0.011	ND	ND	ND	ND	0.053 ± 0.005
	ND	ND	ND	ND	ND	ND
U						
	ND	ND	ND	ND	ND	ND
	ND	ND	ND	ND	ND	ND
	ND	ND	ND	ND	ND	ND
	0.101 ± 0.013	0.595	0.561	0.420	0.541	0.184
	0.699	0.436	0.447	0.725	0.582	1.04
	0.536	ND	ND	ND	ND	ND
	0.677 ± 0.172	ND	ND	ND	ND	1.15
	0.280 ± 0.092	0.376 ± 0.059	ND	0.287 ± 0.063	ND	ND
V			20.3			
	6.96	7.90	9.88	9.66	ND	ND
	10.7	28.9	26.3	21.1	ND	ND
	14.6	53.1	59.0	42.0	38.2	14.3
	4.31	45.5	43.0	36.5	42.1	10.9
	20.6 ± 11.1	15.9	37.7	7.29	4.52	13.7
	11.8	ND	ND	ND	ND	ND
	27.4	ND	ND	ND	ND	26.4
	11.5	18.9	ND	16.0	ND	ND
Al						
	ND	ND	ND	ND	ND	ND
	ND	ND	ND	ND	ND	ND
	ND	ND	ND	ND	ND	ND
	147	471	492	669	334	403
	816	7731	15674	2491	2895	1054
	1058	ND	ND	ND	ND	ND
	727	ND	ND	ND	ND	1070
As						
	27.0	10.3	20.8	9.00	ND	ND
	30.5	25.1	26.5	21.3	ND	ND
	66.7	89.6	109	83.4	72.1	97.7
	71.9	58.6	53.4	57.8	60.9	62.6
	42.9	14.7	38.8	9.69	8.79	35.3
	33.0	ND	ND	ND	ND	ND
	25.9	ND	ND	ND	ND	60.8
	20.5	14.8	ND	11.9	ND	ND
As (III)						
	4.15	0.948 ± 0.160	ND	0.818 ± 0.134	ND	ND
	ND	ND	ND	ND	ND	ND
	ND	ND	ND	ND	ND	ND
	14.2	31.9 ± 3.62	40.1 ± 5.55	1.25 ± 0.240	27.9	175
	11.7	1.73	1.78	2.05	1.60	4.78 ± 0.667
	7.54 ± 0.894	ND	ND	ND	ND	ND
	5.71 ± 0.828	ND	ND	ND	ND	8.57
	5.72	4.36	ND	4.41	ND	ND

BDL: values in bold indicate value below detection limit.
±: standard deviation given where %RSD is greater than 5%.
ND: not determined.
*: measured by spectrophotometry.

Appendix D. Temperature, pH, dissolved oxygen, conductivity, salinity, major solute, and trace element concentrations in groundwaters from Lac des Allemands, Bayou Fortier, and the Mississippi River

		LdA-W1	LdA-W2	LdA-W3	LdA-W4	LdA-W5	LdA-W6
Temperature (°C)							
	Oct-13	24.00	21.80	22.50	ND	23.90	22.60
	Feb-14	20.30	ND	19.70	ND	21.40	21.90
	Apr-14	20.65	19.88	20.56	17.27	18.29	18.54
	May-14	ND	ND	ND	21.60	22.50	ND
	Sep-14	ND	ND	ND	ND	ND	ND
Conductivity ($\mu S\ cm^{-1}$)							
	Oct-13	1727	2110	1127	ND	1582	1517
	Feb-14	1030	ND	995	ND	1345	1451
	Apr-14	1947	2114	1084	2501	1615	308.0
	May-14	ND	ND	ND	2526	1570	ND
	Sep-14	ND	ND	ND	ND	ND	ND
Salinity (psu)							
	Oct-13	0.880	1.15	0.590	ND	0.810	0.810
	Feb-14	0.580	ND	0.550	ND	0.720	0.770
	Apr-14	0.990	1.08	0.540	1.30	0.820	0.150
	May-14	ND	ND	ND	1.31	0.790	ND
	Sep-14	ND	ND	ND	ND	ND	ND
pH							
	Oct-13	7.19	7.08	6.44	6.70	6.62	6.64
	Feb-14	7.61	ND	6.85	7.03	7.18	7.54
	Apr-14	7.30	7.04	5.27	6.80	6.85	6.83
	May-14	ND	ND	ND	6.60	6.45	ND
	Sep-14	ND	ND	ND	7.59	6.74	7.46
DOC ($mmol\ L^{-1}$)							
	Oct-13	3.49	2.55	2.15	3.73	5.52	9.77
	Feb-14	1.78	ND	1.07	2.63	1.58	1.69
	Apr-14	2.37	3.93	1.99	1.39	1.99	0.971
	May-14	ND	ND	ND	1.38	ND	ND
	Sep-14	2.60	ND	ND	3.00	1.09	1.46
TN ($\mu mol\ L^{-1}$)							
	Oct-13	541	577	355	222	468	581
	Feb-14	547	ND	224	117	231	281
	Apr-14	536	1298	275	111	452	71.7
	May-14	ND	ND	ND	168	ND	ND
	Sep-14	655	ND	ND	142	303	114
mmol kg⁻¹							
Mg							
	Oct-13	2.74	2.85	1.87	3.98	2.51	1.91
	Feb-14	2.52	ND	1.68	3.96	2.59	2.26
	Apr-14	2.60	2.47	1.59	3.55	2.35	0.300
	May-14	ND	ND	ND	3.54	2.02	ND
[1]	Sep-14	2.65	ND	ND	3.88	2.37	0.152
Ca							
	Oct-13	1.26	1.24	0.997	3.45	1.26	1.08
	Feb-14	1.14	ND	0.793	4.47	1.76	1.00
	Apr-14	2.29	1.10	1.14	4.24	1.18	0.251
	May-14	ND	ND	ND	3.63	1.08	ND
	Sep-14	1.74	ND	ND	5.65	2.02	0.209
Na							
	Oct-13	10.8	12.3	5.07	8.49	8.37	8.01
	Feb-14	11.1	ND	4.42	8.55	7.76	9.07
	Apr-14	11.1	12.0	4.59	8.46	8.27	1.07
	May-14	ND	ND	ND	7.39	6.37	ND
	Sep-14	11.2	ND	ND	9.35	8.59	0.513
$^{*}SO_4^{2-}$							
	Oct-13	**0.014**	**0.014**	**0.014**	**0.014**	**0.014**	**0.014**
	Feb-14	0.042	ND	**0.014**	0.073	0.031	**0.014**
	Apr-14	**0.014**	**0.014**	**0.014**	**0.014**	**0.014**	**0.014**
	May-14	ND	ND	ND	**0.014**	**0.014**	ND

(*continued on next page*)

(*continued*)

		LdA-W1	LdA-W2	LdA-W3	LdA-W4	LdA-W5	LdA-W6
	Sep-14	6.83	ND	ND	1.42	2.37	2.62
Alkalinity (as HCO_3^-)							
	Oct-13	11.1	9.91	7.19	19.2	11.6	9.03
	Feb-14	15.0	ND	10.1	17.4	10.2	11.4
	Apr-14	10.9	8.88	7.44	13.2	6.96	1.84
	May-14	ND	ND	ND	16.2	8.88	ND
	Sep-14	6.54	ND	ND	17.2	9.69	0.935
µmol kg⁻¹							
K							
	Oct-13	319	375	251	66.5	243	234
	Feb-14	337	ND	253	54.2	294	317
	Apr-14	353	443	438	69.4	255	67.2
	May-14	ND	ND	ND	53.6	249	ND
	Sep-14	363	ND	ND	46.1	267	48.5
Ba							
	Oct-13	1.64	1.19	1.95	5.65	1.89	2.15
	Feb-14	ND	ND	ND	ND	ND	ND
	Apr-14	1.23	1.18	1.29	4.14	1.44	0.400
	May-14	ND	ND	ND	6.30	1.22	ND
	Sep-14	1.18	ND	ND	5.37	2.07	0.339
Sr							
	Oct-13	8.35	7.15	4.81	14.8	6.95	4.98
	Feb-14	8.14	ND	5.84	16.9	8.01	6.79
	Apr-14	7.02	5.74	4.59	13.2	5.92	0.943
	May-14	ND	ND	ND	14.9	5.43	ND
	Sep-14	7.07	ND	ND	13.8	7.12	0.724
Fe							
	Oct-13	60.5	14.8	42.6	84.8	13.1	82.2
	Feb-14	1.14	ND	3.34	5.92	3.61	2.48
	Apr-14	3.81	25.7	14.3	58.4	10.8	6.76
	May-14	ND	ND	ND	131	29.7	ND
	Sep-14	14.8	ND	ND	176	55.5	14.8
*Fe(II)							
	Oct-13	36.3	18.0	39.6	44.6	20.5	42.3
	Feb-14	12.4	ND	0.0898	12.7	15.0	8.95
	Apr-14	2.15	4.30	3.58	14.3	4.30	2.33
	May-14	ND	ND	ND	23.3	2.69	ND
	Sep-14	3.04	ND	ND	26.5	30.1	**0.255**
*Fe_{Total}							
	Oct-13	ND	ND	ND	ND	ND	ND
	Feb-14	43.7	ND	0.022	ND	32.9	32.1
	Apr-14	2.86	0.895	7.52	36.9	11.1	5.01
	May-14	ND	ND	ND	52.8	14.3	ND
	Sep-14	16.5	ND	ND	158	44.4	25.1
Mn							
	Oct-13	11.0	9.05	9.48	36.6	10.3	15.6
	Feb-14	7.41	ND	5.73	39.4	9.48	10.3
	Apr-14	6.92	9.01	8.55	46.2	9.57	1.66
	May-14	ND	ND	ND	46.1	11.0	ND
	Sep-14	7.45	ND	ND	52.9	15.3	1.22
*S(-II)							
	Oct-13	2.71	58.0	8.80	20.8	24.3	28.8
	Feb-14	21.0	ND	17.6	16.0	8.98	9.26
	Apr-14	0.499	0.748	**0.219**	0.156	1.65	0.499
	May-14	ND	ND	ND	0.343	0.343	ND
	Sep-14	1.59	ND	ND	0.998	**0.219**	2.31
nmol kg⁻¹							
Mo							
	Oct-13	2.38	2.727	2.69	4.77	3.04	3.20
	Feb-14	2.63	ND	2.68	4.05	1.45	2.39
	Apr-14	1.44 ± 0.177	61.8	1.03 ± 0.240	2.31	0.536	3.13
	May-14	ND	ND	ND	2.13	0.418	ND
	Sep-14	ND	ND	ND	ND	ND	ND
W							
	Oct-13	0.375	0.139	0.143	0.310	0.136	0.232
	Feb-14	0.175	ND	0.171	0.205	0.096	0.131 ± 0.027
	Apr-14	**0.028**	0.139	**0.028**	0.042	**0.028**	**0.028**
	May-14	ND	ND	ND	0.067	0.120	ND
	Sep-14	ND	ND	ND	ND	ND	ND

(*continued*)

		LdA-W1	LdA-W2	LdA-W3	LdA-W4	LdA-W5	LdA-W6
U							
	Oct-13	0.619	0.482	0.671	1.85 ± 1.13	0.734 ± 0.046	0.829
	Feb-14	1.05 ± 0.517	ND	1.563	1.89	0.308 ± 0.042	1.13 ± 0.962
	Apr-14	0.258 ± 0.050	3.95	0.344	0.385	0.111	0.266
	May-14	ND	ND	ND	0.120	0.0575	ND
	Sep-14	0.194 ± 0.029	ND	ND	0.105 ± 0.017	0.099 ± 0.029	0.153
V							
	Oct-13	16.2	25.9 ± 5.69	21.7 ± 2.96	14.4	14.9	20.9 ± 2.12
	Feb-14	33.0	ND	52.1 ± 23.8	45.1	15.5	27.2
	Apr-14	16.4	97.2	10.5	9.21	5.76	17.6
	May-14	ND	ND	ND	6.36	6.01	ND
	Sep-14	12.6	ND	ND	6.10	5.87	18.0
Al							
	Oct-13	328	1208	1729	827	1095	1732
	Feb-14	818	ND	2021	684	486	569
	Apr-14	534	15941	511 ± 87.1	225 ± 31.4	181	1051
	May-14	ND	ND	ND	142	150	ND
	Sep-14	ND	ND	ND	ND	ND	ND
As							
	Oct-13	8.90	21.5	16.7	26.1	13.8	22.0
	Feb-14	30.0 ± 30.6	ND	18.5	26.1	4.53	8.89
	Apr-14	3.97	81.8	5.19	9.53	4.57	22.7
	May-14	ND	ND	ND	11.1	2.75 ± 0.454	ND
	Sep-14	2.22	ND	ND	9.39	2.50	8.12
As (III)							
	Oct-13	3.27	9.67	8.26	15.1	8.14	10.4
	Feb-14	5.58	ND	8.81	9.44	1.68	3.78
	Apr-14	1.29	33.0	2.32	4.22	1.97	6.32
	May-14	ND	ND	ND	3.13 ± 0.414	0.436	ND
	Sep-14	0.298	ND	ND	1.78	0.128 ± 0.074	1.45

		LdA-W7	LdA-W8	LdA-W9	EDG	VAC-1	VAC-2
Temperature (°C)							
	Oct-13	ND	ND	ND	ND	ND	ND
	Feb-14	ND	ND	ND	ND	ND	ND
	Apr-14	21.44	22.01	18.80	ND	ND	ND
	May-14	ND	ND	24.06	25.50	22.90	27.50
	Sep-14	ND	ND	ND	23.75	27.04	24.27
Conductivity (μS cm^{-1})							
	Oct-13	ND	ND	ND	ND	ND	ND
	Feb-14	ND	ND	ND	ND	ND	ND
	Apr-14	2260	39410	2302	ND	ND	ND
	May-14	ND	ND	2270	1085	526.0	145.0
	Sep-14	ND	ND	ND	772.0	872.0	3036
Salinity (psu)							
	Oct-13	ND	ND	ND	ND	ND	ND
	Feb-14	ND	ND	ND	ND	ND	ND
	Apr-14	1.16	25.2	1.19	ND	ND	ND
	May-14	ND	ND	1.17	0.550	0.240	0.710
	Sep-14	ND	ND	ND	0.380	0.430	1.58
pH							
	Oct-13	ND	ND	ND	ND	ND	ND
	Feb-14	ND	ND	ND	ND	ND	ND
	Apr-14	6.95	6.50	6.93	ND	ND	ND
	May-14	ND	ND	6.73	6.64	7.41	6.88
	Sep-14	6.77	ND	8.21	8.9(Ji)	7.37(Ji)	ND
DOC (mmol L^{-1})							
	Oct-13	ND	ND	ND	ND	ND	ND
	Feb-14	ND	ND	ND	ND	ND	ND
	Apr-14	7.64	2.51	5.50	ND	ND	ND
	May-14	ND	ND	4.69	1.22	3.03	6.59
	Sep-14	1.68	ND	1.94	3.41	5.69	3.77
TN (μmol L^{-1})	Oct-13						
	Oct-13	ND	ND	ND	ND	ND	ND
	Feb-14	ND	ND	ND	ND	ND	ND
	Apr-14	772	1598	261	ND	ND	ND
	May-14	ND	ND	288	64.2	29.4	515
	Sep-14	549	ND	259	67.0	48.7	595

(*continued on next page*)

(*continued*)

		LdA-W7	LdA-W8	LdA-W9	EDG	VAC-1	VAC-2
mmol kg^{-1}							
Mg							
	Oct-13	ND	ND	ND	ND	ND	ND
	Feb-14	ND	ND	ND	ND	ND	ND
	Apr-14	2.17	32.2	2.68	ND	ND	ND
	May-14	ND	ND	3.58	1.27	1.23	3.04
	Sep-14	0.998	ND	3.11	1.26	1.18	3.64
Ca							
	Oct-13	ND	ND	ND	ND	ND	ND
	Feb-14	ND	ND	ND	ND	ND	ND
	Apr-14	1.25	16.0	1.95	ND	ND	ND
	May-14	ND	ND	1.71	1.61	2.12	3.56
	Sep-14	0.878	ND	2.02	2.25	2.54	4.75
Na							
	Oct-13	ND	ND	ND	ND	ND	ND
	Feb-14	ND	ND	ND	ND	ND	ND
	Apr-14	12.3	355	12.8	ND	ND	ND
	May-14	ND	ND	12.7	0.621 ± 0.103	1.20	11.8
	Sep-14	5.67	ND	13.1	0.616	1.36	16.1
*SO_4^{2-}							
	Oct-13	ND	ND	ND	ND	ND	ND
	Feb-14	ND	ND	ND	ND	ND	ND
	Apr-14	**0.014**	**0.014**	**0.014**	ND	ND	ND
	May-14	ND	ND	0.042	0.104	0.021	**0.014**
	Sep-14	1.12		ND	1.17	0.645	2.42
Alkalinity (as HCO_3^-)							
	Oct-13	ND	ND	ND	ND	ND	ND
	Feb-14	ND	ND	ND	ND	ND	ND
	Apr-14	7.36	3.28	11.1	ND	ND	ND
	May-14	ND	ND	15.4	5.12	7.52	19.5
	Sep-14	12.9	ND	10.4	5.09	9.93	21.3
μmol kg^{-1}							
K							
	Oct-13	ND	ND	ND	ND	ND	ND
	Feb-14	ND	ND	ND	ND	ND	ND
	Apr-14	0	0	0	ND	ND	ND
	May-14	ND	ND	391	128	68.5	213
	Sep-14	157	ND	359	126	51.0	237
Ba							
	Oct-13	ND	ND	ND	ND	ND	ND
	Feb-14	ND	ND	ND	ND	ND	ND
	Apr-14	2.27	84.5	2.12	ND	ND	ND
	May-14	ND	ND	2.39	2.15	2.26	6.28
	Sep-14	1.02	ND	2.17	2.31	1.95	7.58
Sr							
	Oct-13	ND	ND	ND	ND	ND	ND
	Feb-14	ND	ND	ND	ND	ND	ND
	Apr-14	5.61	91.5	7.05	ND	ND	ND
	May-14	ND	ND	10.2	8.18 ± 2.86	6.36 ± 0.754	13.8
	Sep-14	3.35	ND	7.98	4.89	5.51	14.3
Fe							
	Oct-13	ND	ND	ND	ND	ND	ND
	Feb-14	ND	ND	ND	ND	ND	ND
	Apr-14	9.38	268	58.7	ND	ND	ND
	May-14	ND	ND	87.0	5.67	0.129	57.1
	Sep-14	45.4	ND	30.1	32.2	47.0	414
*Fe(II)							
	Oct-13	ND	ND	ND	ND	ND	ND
	Feb-14	ND	ND	ND	ND	ND	ND
	Apr-14	3.22	7914	88.1	ND	ND	ND
	May-14	ND	ND	2.51	6.09	4.66	10.9
	Sep-14	6.45	ND	4.83	15.8	43.3	26.0
*Fe_{Total}							
	Oct-13	ND	ND	ND	ND	ND	ND
	Feb-14	ND	ND	ND	ND	ND	ND
	Apr-14	6.27	180	44.8	ND	ND	ND
	May-14	ND	ND	36.3	20.4	8.42	36.7
	Sep-14	101	ND	25.2	82.7	56.6	82.7

(*continued*)

		LdA-W7	LdA-W8	LdA-W9	EDG	VAC-1	VAC-2
Mn							
	Oct-13	ND	ND	ND	ND	ND	ND
	Feb-14	ND	ND	ND	ND	ND	ND
	Apr-14	23.1	97.3	19.7	ND	ND	ND
	May-14	ND	ND	17.5	50.8	7.88	57.6
	Sep-14	6.92	ND	13.4	53.5	37.2	46.3
*S(-II)							
	Oct-13	ND	ND	ND	ND	ND	ND
	Feb-14	ND	ND	ND	ND	ND	ND
	Apr-14	0.031	1.47	0.343	ND	ND	ND
	May-14	ND	ND	0.967	4.18	2.65	1.15
	Sep-14	**0.219**	ND	0.156	8.27	2.53	0.218
nmol kg^{-1}							
Mo							
	Oct-13	ND	ND	ND	ND	ND	ND
	Feb-14	ND	ND	ND	ND	ND	ND
	Apr-14	3.26	6.52	2.26	ND	ND	ND
	May-14	ND	ND	1.39	54.7	95.6	53.9
	Sep-14	ND	ND	ND	ND	ND	ND
W							
	Oct-13	ND	ND	ND	ND	ND	ND
	Feb-14	ND	ND	ND	ND	ND	ND
	Apr-14	0.057	0.091	0.080	ND	ND	ND
	May-14	ND	ND	0.040	0.153	0.327	0.537
	Sep-14	ND	ND	ND	ND	ND	ND
U							
	Oct-13	ND	ND	ND	ND	ND	ND
	Feb-14	ND	ND	ND	ND	ND	ND
	Apr-14	2.00	2.39	0.665	ND	ND	ND
	May-14	ND	ND	0.165	9.03	27.8	7.86
	Sep-14	0.205 ± 0.029	ND	0.052	3.56	4.68	0.412
V							
	Oct-13	ND	ND	ND	ND	ND	ND
	Feb-14	ND	ND	ND	ND	ND	ND
	Apr-14	16.7	12.5	11.9	ND	ND	ND
	May-14	ND	ND	14.1	16.1	62.7	44.4
	Sep-14	18.1	ND	14.9	4.77	8.80	23.8
Al							
	Oct-13	ND	ND	ND	ND	ND	ND
	Feb-14	ND	ND	ND	ND	ND	ND
	Apr-14	575	36.6 ± 17.3	31.1	ND	ND	ND
	May-14	ND	ND	214	**7.07**	88.0	13.6 ± 1.22
	Sep-14	ND	ND	ND	ND	ND	ND
As							
	Oct-13	ND	ND	ND	ND	ND	ND
	Feb-14	ND	ND	ND	ND	ND	ND
	Apr-14	17.9	11.2	11.8	ND	ND	ND
	May-14	ND	ND	7.61	216	55.8	186
	Sep-14	9.21	ND	2.47	298	327	418
As (III)							
	Oct-13	ND	ND	ND	ND	ND	ND
	Feb-14	ND	ND	ND	ND	ND	ND
	Apr-14	8.39	9.65	8.53 ± 0.974	ND	ND	ND
	May-14	ND	ND	1.52	146	19.3	93.3
	Sep-14	0.932	ND	0.254	10.9	53.2	161

BDL: values in bold indicate value below detection limit.
±: standard deviation given where %RSD is greater than 5%.
ND: not determined.
*: measured by spectrophotometry.

Appendix E. Aqueous speciation of trace element species modeled at equilibrium shown as percent of total trace element concentration

%	MoO_4^{2-}	MoS_4^{2-}	$MoOS_3^{2-}$	$MoO_2S_2^{2-}$	MoO_3S^{2-}	$FeOOHMoS_4^{3-}$
LdAW1-Oct	87.8				11.6	
LDAW2-Oct	2.3	41.2	7.5	10.7	24.1	14.1
LdAW3-Oct	36.1	4.6	9.4	14.5	35.2	
LdAW4-Oct	12.5	21.2	22.4	18.0	22.8	3.0
LdAW5-Oct	7.2	32.1	26.7	16.9	16.9	
LdAW6-Oct	4.6	37.8	27.0	14.6	12.6	3.5
LdAW1-Feb	60.8		2.1	6.3	29.9	
LdAW3-Feb	22.8		16.5	18.0	31.1	
LdAW4-Feb	36.4	4.7	9.4	14.4	34.7	
LdAW5-Feb	63.6		1.7	5.5	28.6	
LdAW6-Feb	77.7			2.1	19.6	
LdAW1-April	98.1				2.0	
LDAW2-April	96.3				3.6	
LdAW3-April	91.0				2.9	
LdAW4-April	98.6				1.1	
LdAW5-April	87.9				11.3	
LdAW6-April	96.0				3.9	
LdAW7-April	99.6					
LdAW8-April	90.1				9.1	
LdAW9-April	97.8				2.3	
LdAW4-May	96.6				3.0	
LdAW5-May	96.1				3.6	
LdAW9-May	92.4				7.5	
EDG-May	68.0		1.1	4.2	26.3	
VACW1-May	91.4				8.3	
VACW2-May	93.8				6.0	

%	WO_4^{2-}	WO_3S^{2-}
LdAW1-Oct	99.7	
LDAW2-Oct	97.2	2.8
LdAW3-Oct	99.2	
LdAW4-Oct	98.2	1.6
LdAW5-Oct	98.0	2.0
LdAW6-Oct	97.7	2.3
LdAW1-Feb	99.7	
LdAW3-Feb	98.9	1.2
LdAW4-Feb	99.3	
LdAW5-Feb	99.6	
LdAW6-Feb	99.9	
LdAW1-April	100.1	
LDAW2-April	100.1	
LdAW3-April	98.6	
LdAW4-April	99.9	
LdAW5-April	100.0	
LdAW6-April	99.9	
LdAW7-April	99.9	
LdAW8-April	99.9	
LdAW9-April	100.0	
LdAW4-May	99.9	
LdAW5-May	100.0	
LdAW9-May	99.8	
EDG-May	99.7	
VACW1-May	100.0	
VACW2-May	99.9	

%	AsS_4^{3-}	H_3AsO_3	$H_2AsS_3^-$	$HAsS_3O^{2-}$	$H_2AsSO_2^-$	$HAsSO_3^{2-}$	$H_2AsSO_3^-$	$HAsS_2O_2^{2-}$	$H2AsS_2O_2^-$	$HAsO_4^{-}$	$H_2AsO_3^-$	$H_2AsO_4^-$
LdAW1-Oct	15.1	36.1		47.4								
LDAW2-Oct	47.2	30.3	8.1	7.4	5.2							
LdAW3-Oct	13.1	48.8		36.8								
LdAW4-Oct	25.4	54.3	1.0	16.3	2.2							
LdAW5-Oct	23.9	54.7	1.7	16.5	2.3							
LdAW6-Oct	32.8	42.5	2.2	19.3	2.1							
LdAW1-Feb	61.1	16.6		20.0	1.4							
LdAW3-Feb	30.5	44.9		21.7	1.8							
LdAW4-Feb	40.8	34.1		22.6	1.6							
LdAW5-Feb	31.5	35.7		30.9	1.0							
LdAW6-Feb	32.0	40.1		25.2	1.5							
LdAW1-April	3.0	31.9		47.0		10.5	5.2	1.2				
LDAW2-April	3.1	40.0		49.0		3.2	3.0					
LdAW3-April		44.7		7.3			40.9	6.0				
LdAW4-April		44.1		20.2		13.2	20.0	1.1				

(*continued*)

%	AsS_4^{3-}	H_3AsO_3	$H_2AsS_3^-$	$HAsS_3O^{2-}$	$H_2AsSO_2^-$	$HAsSO_3^{2-}$	$H_2AsSO_3^-$	$HAsS_2O_2^{2-}$	$H2AsS_2O_2^-$	$HAsO_4^{-}$	$H_2AsO_3^-$	$H_2AsO_4^-$
LdAW5-April	6.5	42.6		49.2								
LdAW6-April	1.4	27.7		57.4		3.8	7.4	1.3				
LdAW7-April		46.6				24.0	27.4					
LdAW8-April	3.1	85.5		10.7								
LdAW9-April		71.6		19.5		3.2	3.8					
LdAW4-May	1.1	28.5		51.3		4.7	11.6	1.7				
LdAW5-May		15.9		60.0		4.1	15.6	2.7				
LdAW9-May	5.2	19.8		70.9			1.7					
EDG-May	5.4	66.7		26.9								
VACW1-May	14.4	33.6		49.7								
VACW2-May	3.6	49.8		43.3			1.2					
LDAW1-Sept	15.5	13.1		66.2		2.9						
LdAW4-Sept	9.4	18.4		57.9		9.8	2.3	1.3				
LdAW5-Sept		4.9		51.1		13.8	25.7	1.5	2.2			
LdAW6-Sept	16.4	10.1		63.6		1.1		1.4	2.1			
LdAW7-Sept				45.0		14.1	26.5					
LdAW9-Sept		9.3				81.0	4.9			2.0	1.0	
EDG-Sept	37.9	2.4		31.1			24.3	1.5			1.2	
VACW1-Sept	14.1	15.9		66.4			1.7					
VACW2-Sept		38.0				27.4	24.8			6.2		3.4

sample	VO^{2+}	$V(OH)_2^+$	HVO_4^{2-}	sample	VO^{2+}	$V(OH)_2^+$	HVO_4^{2-}
LdAW1-Oct	99.7			**LdAW4-May**	98.5	1.5	
LDAW2-Oct	99.8			**LdAW5-May**	97.6	2.2	
LdAW3-Oct	98.2	1.8		**LdAW9-May**	99.3		
LdAW4-Oct	98.9	1.2		**EDG-May**	99.4		
LdAW5-Oct	98.6	1.5		**VACW1-May**	99.9		
LdAW6-Oct	98.9	1.2		**VACW2-May**	99.6		
LdAW1-Feb	99.9			**LDAW1-Sept**	100.3		
LdAW3-Feb	99.5			**LdAW4-Sept**	99.9		
LdAW4-Feb	99.9			**LdAW5-Sept**	99.4		
LdAW5-Feb	99.8			**LdAW6-Sept**	99.9		
LdAW6-Feb	99.9			**LdAW7-Sept**	98.1	2.1	
LdAW1-April	99.7			**LdAW9-Sept**	100.2		
LDAW2-April	99.9			**EDG-Sept**	97.9		1.7
LdAW3-April	58.4	34.3		**VACW1-Sept**	99.9		
LdAW4-April	99.4						
LdAW5-April	99.0						
LdAW6-April	99.7						
LdAW7-April	100.0						
LdAW8-April	97.6	2.2					
LdAW9-April	99.3						

Appendix F. Mineral saturation states (log Q/K) of Lac des Allemands groundwaters for sulfide-bearing minerals

Sample	Pyrite	Mackinawite	Realgar	Sample	Pyrite	Mackinawite	Realgar
LdAW1-Oct	6.93	0.37	−4.74	**LdAW4-May**	5.25	−1.12	−5.59
LDAW2-Oct	8.60	0.94	−2.88	**LdAW5-May**	4.60	−1.92	−6.42
LdAW3-Oct	7.25	−0.35	−3.56	**LdAW9-May**	6.12	−3.45	−5.47
LdAW4-Oct	8.29	0.65	−2.92	**EDG-May**	6.21	−1.20	−2.83
LdAW5-Oct	7.62	−0.16	−3.11	**VACW1-May**	4.41	−1.96	−4.14
LdAW6-Oct	8.59	0.76	−2.94	**VACW2-May**	5.83	−0.63	−3.70
LdAW1-Feb	6.93	0.03	−3.86	**LDAW1-Sept**	6.55	−0.18	−6.56
LdAW3-Feb	6.97	−0.53	−3.28	**LdAW4-Sept**	7.05	0.79	−5.99
LdAW4-Feb	7.30	−0.14	−3.44	**LdAW5-Sept**	5.26	−1.44	−7.49
LdAW5-Feb	6.72	−0.33	−4.48	**LdAW6-Sept**	6.94	0.10	−5.62
LdAW6-Feb	6.56	−0.03	−4.30	**LdAW7-Sept**	5.14	−1.46	−6.63
LdAW1-April	4.45	−1.44	−6.03	**LdAW9-Sept**	4.77	−0.09	−8.20
LDAW2-April	5.38	−0.84	−4.39	**EDG-Sept**	7.69	2.32	−5.44
LdAW3-April	2.43	−4.63	−6.07	**VACW1-Sept**	6.91	0.28	−4.08
LdAW4-April	4.45	−1.50	−5.89	**VACW2-Sept**	2.53	−2.35	−6.81
LdAW5-April	5.69	−1.03	−5.06				
LdAW6-April	4.71	−1.67	−5.18				
LdAW7-April	2.36	−2.86	−6.58				
LdAW8-April	6.07	−0.72	−4.29				
LdAW9-April	5.19	−0.92	−5.22				

References

Adelson, J.M., Helz, G.R., Miller, C.V., 2001. Reconstructing the rise of recent coastal anoxia; molybdenum in Chesapeake Bay sediments1. Geochem. Cosmochim. Acta 65 (2), 237–252.

Alewell, C., Paul, S., Lischeid, G., Storck, F.R., 2008. Co-regulation of redox processes in freshwater wetlands as a function of organic matter availability? Sci. Total Environ. 404, 335–342.

Algeo, T.J., Lyons, T.W., 2006. Mo-total organic carbon covariation in modern anoxic marine environments: implications for analysis of paleoredox and paleohydrographic conditions. Paleoceanography 21.

Arnórsson, S., Óskarsson, N., 2007. Molybdenum and tungsten in volcanic rocks and in surface and <100°C ground waters in Iceland. Geochem. Cosmochim. Acta 71, 284–304.

Baes, C.F., Mesmer, R.E., 1976. Hydrolysis of Cations. Wiley, New York.

Beck, M., Dellwig, L., Schnetger, B., Brumsack, H.J., 2008. Cycling of trace metals (Mn, Fe, Mo, U, V, Cr) in deep pore waters of intertidal flat sediments. Geochem. Cosmochim. Acta 72 (12), 2822–2840.

Berner, R.A., 1981. A new geochemical classification of sedimentary environments. J. Sediment. Res. 51 (2).

Bertine, K.K., Turekian, K.K., 1973. Molybdenum in marine deposits. Geochem. Cosmochim. Acta 37, 1415–1434.

Bethke, C., 2008. Geochemical and Biogeochemical Reaction Modeling. Cambridge University Press, Cambridge.

Bianchi, T.S., Allison, M.A., 2009. Large-river delta-front estuaries as natural "recorders" of global environmental change. Proc. Natl. Acad. Sci. Unit. States Am. 106 (20), 8085–8092.

Bone, S.E., Gonneea, M.E., Charette, M.A., 2006. Geochemical cycling of arsenic in a coastal aquifer. Environ. Sci. Technol. 40, 3273–3278.

Bostick, B.C., Chen, C., Fendorf, S., 2004. Arsenite retention mechanisms within estuarine sediments of Pescadero, CA. Environ. Sci. Technol. 38 (12), 3299–3304.

Breaux, A.M., 2015. Utilization of Shallow Seismic, Resistivity Profiling, and Sediment Core Analyses for Identification of Semi-permeable Sediments that Act as Conduits for Submarine Groundwater Discharge, Barataria Bay, Louisiana. Master's Thesis. Tulane University.

Breit, G.N., Wanty, R.B., 1991. Vanadium accumulation in carbonaceous rocks—a review of geochemical controls during deposition and diagenesis. Chem. Geol. 91 (2), 83–97.

Burton, E.D., Johnston, S.G., Planer-Friedrich, B., 2013. Coupling of arsenic mobility to sulfur transformations during microbial sulfate reduction in the presence and absence of humic acid. Chem. Geol. 343, 12–24.

Catallo, J.W., Schlenker, M., Gambrell, R.P., Shane, B.S., 1995. Toxic chemicals and trace metals from urban and rural Louisiana lakes: recent historical profiles and toxicological significance. Environ. Sci. Technol. 29, 1436–1445.

Chmura, G.L., Anisfeld, S.C., Cahoon, D.R., Lynch, J.C., 2003. Global carbon sequestration in tidal, saline wetland soils. Global Biogeochem. Cycles 17 (4).

Clarke, M.B., Helz, G.R., 2000. Metal-thiometalate transport of biologically active trace elements in sulfidic environments. 1. Experimental evidence for copper thioarsenate complexing. Environ. Sci. Technol. 34, 1477–1482.

Cline, J.D., 1969. Spectrophotometric determination of hydrogen sulfide in natural water. Limnol. Oceanogr. 14, 454–458.

CRMS, 2015. Coastwide Reference Monitoring System and Coastal Protection and Restoration Authority of Louisiana, Coastwide Reference Monitoring System-wetlands Monitoring Data. Retrieved from Coastal Information Management System (CIMS) database http://cims.coastal.louisiana.gov.

Coleman, J.M., 1988. Dynamic changes and processes in the Mississippi River delta. Geol. Soc. Am. Bull. 100, 999–1015.

Couture, R.M., Rose, J., Kumar, N., Mitchell, K., Wallschlager, D., Van Cappellen, P., 2013. Sorption of arsenite, arsenate, and thioarsenates to iron oxides and iron S(-II)s: a kinetic and spectroscopic investigation. Environ. Sci. Technol. 47, 5652–5659.

Couvillion, B.R., Barras, J.A., Steyer, G.D., Sleaven, W., Fischer, M., Beck, H., Trahan, N., Griffin, B., Heckman, D., 2011. Land Area Change in Coastal Louisiana from 1932 to 2010. U.S. Geological Survey Scientific Investigations Map 3164, scale 1:265, 000, 12 p. pamphlet.

Crusius, J., Calvert, S., Pedersen, T., Sage, D., 1996. Rhenium and molybdenum enrichments in sediments as indicators of oxic, suboxic and sulfidic conditions of deposition. Earth Planet Sci. Lett. 145, 65–78.

Cruywagen, J., 2000. Protonation, oligomerization, and condensation reactions of vanadate(V), molybdate(VI), and tungstate(VI). Advanced Inorganic Chemistry 49, 127–182.

Cullen, W.R., Reimer, K.J., 1989. Arsenic speciation in the environment. Chem. Rev. 89, 713–764.

Dahl, T.W., Chappaz, A., Fitts, J.P., Lyons, T.W., 2013. Molybdenum reduction in a sulfidic lake: evidence from X-ray absorption fine-structure spectroscopy and implications for the Mo paleoproxy. Geochem. Cosmochim. Acta 103, 213–231.

Davison, W., 1993. Iron and manganese in water. Earth Sci. Rev. 34, 1119–1163.

Day Jr., J.W., Boesch, D.F., Clairain, E.J., Kemp, G.P., Laska, S.B., Mitsch, W.J., Orth, K., Mashriqui, H., Reed, D.J., Shabman, L., Simenstad, C.A., Streever, B.J., Twilley, R.R., Watson, C.C., Wells, J.T., Whigham, D.F., 2007. Restoration of the Mississippi delta: lessons from hurricanes katrina and rita. Science 315, 1679–1684.

Delany, J.M., Lundeen, S.R., 1990. The LLNL Thermochecmial Database. Lawrence Livermore National Laboratory. Lawrence Livermore National Laboratory Report UCRL-21658.

DeLaune, R.D., Devai, I., Crozier, C.R., Kelle, P., 2002a. Sulfate reduction in Louisiana marsh soils of varying salinities. Commun. Soil Sci. Plant Anal. 33, 79–94.

DeLaune, R.D., Devai, I., Lindau, C.W., 2002b. Flux of reduced sulfur gases along a salinity gradient in Louisiana coastal marshes. Estuar. Coast Shelf Sci. 54 (6), 1003–1011.

Dos Santos Afonso, M., Stumm, W., 1992. Reductive dissolution of iron (III) (hydr) oxides by hydrogen sulfide. Langmuir 8 (6), 1671–1675.

Eary, L.E., 1992. The solubility of amorphous As2S3 from 25 to 90oC. Geochem. Cosmochim. Acta 56, 2267–2280.

Eaton, A.D., Clesceri, L.S., Greenberg, A.E., 1995a. IRON (3500-Fe)/Phenanthroline Method. Standard Methods for the Examination of Water and Waste Water, nineteenth ed. American Public Health Association, Washington, DC, pp. 3–68. – 3–70.

Eaton, A.D., Clesceri, L.S., Greenberg, A.E., 1995b. SULFIDE (4500-S2−)/Methylene Blue Method. Standard Methods for the Examination of Water and WasteWater, nineteenth ed. American Public Health Association, Washington, DC, pp. 4–122. – 4–123.

Eaton, A.D., Clesceri, L.S., Rice, E.W., Greenberg, A.E., Franson, M.A.H.A., 2005. APHA: Standard Methods for the Examination of Water and Wastewater. Centennial Edition. APHA, AWWA, WEF, Washington, DC.

Emerson, S.R., Huested, S.S., 1991. Ocean anoxia and the concentrations of molybdenum and vanadium in seawater. Mar. Chem. 34 (3-4), 177–196.

Erickson, B.E., Helz, G.R., 2000. Molybdenum(VI) speciation in sulfidic waters: stability and lability of thiomolybdates. Geochem. Cosmochim. Acta 64, 1149–1158.

Feijtel, T.C., DeLaune, R.D., Patrick Jr., W.H., 1988. Seasonal pore water dynamics in marshes of Barataria Basin, Louisiana. Soil Sci. Soc. Am. J. 52 (1), 59–67.

Ficklin, W.H., 1983. Separation of arsenic(III) and Arsenic(V) in ground waters by ion-exchange. Talanta 30.

Fisk, H.N., McFarlan Jr., E., Kolb, C.R., Wilbert Jr., L.J., 1954. Sedimentary framework of the modern Mississippi delta. J. Sediment. Res. 24.

Froelich, P., Klinkhammer, G.P., Bender, M.A.A., Luedtke, N.A., Heath, G.R., Cullen, D., Maynard, V., 1979. Early oxidation of organic matter in pelagic sediments of the eastern equatorial Atlantic: suboxic diagenesis. Geochem. Cosmochim. Acta 43 (7), 1075–1090.

Gustafsson, J.P., 2003. Modelling molybdate and tungstate adsorption to ferrihydrite. Chem. Geol. 200 (1), 105–115.

Haque, S., Johannesson, K.H., 2006. Arsenic concentrations and speciation along a groundwater flow path: the Carrizo Sand aquifer, Texas, USA. Chem. Geol. 228 (1–3), 57–71.

Helz, G.R., Miller, C.V., Charnock, J.M., Mosselmans, J.F.W., Patrick, R.A.D., Garner, C.D., Vaughan, D.J., 1996. Mechanism of molybdenum removal from the sea and its concentration in black shales: EXAFS evidence. Geochem. Cosmochim. Acta 60 (19), 3631–3642.

Helz, G.R., Tossell, J.A., 2008. Thermodynamic model for arsenic speciation in sulfidic waters: a novel use of ab initio computations. Geochem. Cosmochim. Acta 72, 4457–4468.

Helz, G.R., Bura-Nakić, E., Mikac, N., Ciglenečki, I., 2011. New model for molybdenum behavior in euxinic waters. Chem. Geol. 284, 323–332.

Helz, G.R., Erickson, B.E., Vorlicek, T.P., 2014. Stabilities of thiomolybdate complexes of iron; implications for retention of essential trace elements (Fe, Cu, Mo) in sulfidic waters. Metallomics 6, 1131–1140.

Hingston, F.J., Atkinson, R.J., Posner, A.M., Quirk, J.P., 1967. Specific adsorption of anions. Nature 215, 1459–1461.

Inoue, M., Park, D., Justic, D., Wiseman, W.J., 2008. A high-resolution integrated hydrology-hydrodynamic model of the Barataria Basin system. Environ. Model. Software 23, 1122–1132.

Jay, J.A., Blute, N.K., Hemond, H.F., Durant, J.L., 2004. Arsenic-sulfides confound anion exchange resin speciation of aqueous arsenic. Water Res. 38, 1155–1158.

Johannesson, K.H., Tang, J.W., Daniels, J.M., Bounds, W.J., Burdige, D.J., 2004. Rare earth element concentrations and speciation in organic-rich blackwaters of the Great Dismal Swamp, Virginia, USA. Chem. Geol. 209, 271–294.

Kashiwabara, T., Takahashi, Y., Uruga, T., Tanida, H., Terada, Y., Niwa, Y., Nomura, M., 2010. Speciation of tungsten in natural ferromanganese oxides using wavelength dispersive XAFS. Chem. Lett. 39 (8), 870–871.

Kashiwabara, T., Takahashi, Y., Marcus, M.A., Uruga, T., Tanida, H., Terada, Y., Usui, A., 2013. Tungsten species in natural ferromanganese oxides related to its different behavior from molybdenum in oxic ocean. Geochem. Cosmochim. Acta 106, 364–378.

Kemp, G.P., Day, J.W., Freeman, A.M., 2014. Restoring the sustainability of the Mississippi River Delta. Ecol. Eng. 65, 131–146.

Kim, 2015. Investigating Groundwater Inputs to Mississippi River Deltaic Wetlands Using Spatial and Temporal Responses of the Geochemical Tracer, 222Rn. Master's Thesis. University of North Carolina, Chapel Hill.

Kirk, M.F., Holm, T.R., Park, J., Jin, Q.S., Sanford, R.A., Fouke, B.W., Bethke, C.M., 2004. Bacterial sulfate reduction limits natural arsenic contamination in groundwater. Geology 32, 953–956.

Kirk, M.F., Roden, E.E., Crossey, L.J., Brearley, A.J., Spilde, M.N., 2010. Experimental analysis of arsenic precipitation during microbial sulfate and iron reduction in model aquifer sediment reactors. Geochem. Cosmochim. Acta 74, 2538–2555.

Kolker, A.S., Cable, J.E., Johannesson, K.H., Allison, M.A., Inniss, L.V., 2013. Pathways and processes associated with the transport of groundwater in deltaic systems. J. Hydrol. 498, 319–334.

Kosters, E.C., Chmura, G.L., Bailey, A., 1987. Sedimentary and botanical factors influencing peat accumulation in the Mississippi Delta. J. Geol. Soc. 144 (3), 423–434.
Kostka, J.E., Luther, G.W., 1995. Seasonal cycling of Fe in salt marsh sediments. Biogeochemistry 29, 159–181.
Koutsospyros, A., Braida, W., Christodoulatos, C., Dermatas, D., Strigul, N., 2006. A review of tungsten: from environmental obscurity to scrutiny. J. Hazard Mater. 136 (1), 1–19.
Krairapanond, N., Delaune, R.D., Patrick, W.H., 1992. Distribution of organic and reduced sulfur forms in marsh soils of coastal Louisiana. Org. Geochem. 18, 489–500.
Lanesky, D.E., Logan, B.W., Brown, R.G., Hine, A.G., 1979. A new approach to portable vibracoring underwater and on land. J. Sediment. Petrol. 49 (2), 654–657.
Lovley, D.R., 1987. Organic matter mineralization with the reduction of ferric iron – a review. Geomicrobiol. J. 5, 375–399.
Lu, X., Johnson, W.D., Hook, J., 1998. Reaction of vanadate with aquatic humic substances: an ESR and ^{51}V NMR study. Environ. Sci. Technol. 32 (15), 2257–2263.
Martin, J.M., Whitfield, M., 1983. The significance of the river input of chemical elements to the ocean. In: Wong, C.S., Boyle, E., Bruland, K.W., Burton, J.D., Goldberg, E.D. (Eds.), Trace Metals in Seawater. Plenum Press, New York, pp. 265–296.
McBride, M.B., 1979. Mobility and reactions of VO^{2+} on hydrated smectite surfaces. Clay Clay Miner. 27 (2), 91–96.
McMahon, P.B., Chapelle, F.H., 2008. Redox processes and water quality of selected principal aquifer systems. Ground Water 46 (2), 259–271.
Mohajerin, T.J., Helz, G.R., White, C.D., Johannesson, K.H., 2014. Tungsten speciation in sulfidic waters: determination of thiotungstate formation constants and modeling their distribution in natural waters. Geochem. Cosmochim. Acta 144, 157–172.
Mohajerin, T.J., Helz, G.R., Johannesson, K.H., 2016. Tungsten-Molybdenum fractionation in estuarine environments. Geochem. Cosmochim. Acta 177, 105–119.
Mongenot, T., Tribovillard, N.-P., Arbey, F., Lallier-Verges, M., Derenne, S., Largeau, Cl, Connan, J., 2000. Microbial mat development and iron deficiency: intertwined key factors in the formation of organic and sulphur-rich deposits. Bull. Soc. Geol. Fr. 171, 23–36.
Morse, J.W., Millero, F.J., Cornwell, J.C., Rickard, D., 1987. The chemistry of hydrogen sulfide and iron sulfide systems in natural waters. Earth Sci. Rev. 24, 1–42.
Neubauer, S.C., Givler, K., Valentine, S., Megonigal, J.P., 2005. Seasonal patterns and plant-mediated controls of suburface wetland biogeochemistry. Ecology 86, 3334–3344.
Nordstrom, D.K., Archer, D.G., 2003. Arsenic thermodynamic data and environmental geochemistry. In: Welch, A.H., Stollenwerk, K.G. (Eds.), Arsenic in Groundwater: Geochemistry and Occurrence. Kluwer Academic Press, Boston, pp. 1–25.
Nordstrom, D.K., Majzlan, J., Königsberger, E., 2014. Thermodynamic properties for arsenic minerals and aqueous species. Rev. Mineral. Geochem. 79 (1), 217–255.
Nyman, J.A., Delaune, R.D., Patrick Jr., W.H., 1990. Wetland soils formation in the rapidly subsiding Mississippi River Deltaic Plain: mineral and organic matter relationships. Estuar. Coast Shelf Sci. 31, 57–69.
O'Connor, A.E., Luek, J.L., McIntosh, H., Beck, A.J., 2015. Geochemistry of redox-sensitive trace elements in a shallow subterranean estuary. Mar. Chem. 172, 70–81.
Olesik, 2014. Inductively Coupled Plasma Mass Spectrometers. Treatise on Geochemistry, , second ed.vol. 15, pp. 209–336
Paola, C., Twilley, R.R., Edmonds, D.A., Kim, W., Mohrig, D., Parker, G., Viparelli, E., Voller, V.R., 2011. Natural processes in delta restoration: application to the Mississippi delta. Annual Review of Marine Science 23, 67–91.
Planer-Friedrich, B., London, J., McCleskey, R.B., Nordstrom, D.K., Wallschläger, D., 2007. Thioarsenates in geothermal waters of Yellowstone National Park: determination, preservation, and geochemical importance. Environ. Sci. Technol. 41, 5245–5251.
Pourret, O., Dia, A., Gruau, G., Davranche, M., Bouhnik-Le Coz, M., 2012. Assessment of vanadium distribution in shallow groundwaters. Chem. Geol. 294–295, 89–102.
Reed, D.J., 2002. Sea-level rise and coastal marsh sustainability: geological and ecological factors in the Mississippi delta plain. Geomorphology 48 (1-3), 233–243.
Ren, L., Rabalais, N.N., Turner, R.E., Morrison, W., Mendenhall, W., 2009. Nutrient limitation on phytoplankton growth in the upper Barataria Basin, Louisiana: microcosm bioassays. Estuar. Coast 32, 958–974.
Rickard, D., Griffith, A., Oldroyd, A., Butler, I.B., Lopez-Capel, E., Manning, D.A.C., Apperley, D.C., 2006. The composition of nanoparticulate mackinawite, tetragonal iron(II) monosul- fide. Chem. Geol. 235, 286–298.
Roberts, H.H., 1997. Dynamic changes of the Holocene Mississippi River delta plain: the delta cycle. J. Coast Res. 605–627.
Santos, I.R., Machado, M.I., Niencheski, L.F., Burnett, W., Milani, I.B., Andrade, C.F., Peterson, R.N., Chanton, J., Baisch, P., 2008. Major ion chemistry in a freshwater coastal lagoon from southern Brazil (Mangueira Lagoon): Influence of groundwater inputs. Aquat. Geochem. 14 (2), 133–146.
Schoonen, M.A.A., Barnes, H.L., 1991. Reactions forming pyrite and marcasite from solutions: II. Via FeS precursors below 100 C. Geochem. Cosmochim. Acta 55, 1505–1514.
Seybold, H., Andrade, J.S., Herrmann, H.J., 2007. Modeling river delta formation. Proc. Natl. Acad. Sci. U. S. A. 104, 16804–16809.
Shiller, A.M., 1997. Dissolved trace elements in the MSR: seasonal, interannual, and decadal variability. Geochem. Cosmochim. Acta 61, 4321–4330.
Shiller, A.M., Boyle, E.A., 1987. Dissolved vanadium in rivers and estuaries. Earth Planet Sci. Lett. 86 (2–4), 214–224.
Smedley, P.L., Kinniburgh, D.G., 2002. A review of the source, behaviour and distribution of arsenic in natural waters. Appl. Geochem. 17, 517–568.
Steudel, R., 1996. Mechanism for the formation of elemental sulfur from aqueous sulfide in chemical and microbiological desulfurization processes. Ind. Eng. Chem. Res. 35, 1417–1423.
Stumm, W., Morgan, J., 1996. Aquatic Chemistry: Chemical Equilibria and Rates in Natural Waters, third ed. John Wiley & Sons, New York.
Sundby, B., Vale, C., Caetano, M., Luther, G.W., 2003. Redox chemistry in the root zone of a salt marsh sediment in the Tagus Estuary, Portugal. Aquat. Geochem. 9, 257–271.
Swarzenski, C.M., Doyle, T.W., Fry, B., Hargis, T.G., 2008. Biogeochemical response of organic-rich freshwater marshes in the Louisiana delta plain to chronic river water influx. Biogeochemistry 90, 49–63.
Törnqvist, T.E., Kidder, T.R., Autin, W.J., van der Borg, K., de Jong, A.F., Klerks, C.J., Snijders, E.M.A., Storms, J.E.A., van Dam, R.L., Wiemann, M.C., 1996. A revised chronology for Mississippi River subdeltas. Science 273 (5282), 1693–1696.
Tribovillard, N., Riboulleau, A., Lyons, T., 2004. Enhanced trapping of molybdenum by sulfurized marine organic matter of marine origin in Mesozoic limestones and shales. Chem. Geol. 213, 385–401.
Tribovillard, N., Algeo, T.J., Lyons, T., Riboulleau, A., 2006. Trace metals as paleoredox and paleoproductivity proxies: an update. Chem. Geol. 232, 12–32.
Van der Weijden, C.H., Middelburg, J.J., Delange, G.J., Vandersloot, H.A., Hoede, D., Woittiez, J.R.W., 1990. Profiles of the redox-sensitive trace elements as, Sb, V, Mo and U in the tyro and bannock basins (eastern mediterranean). Mar. Chem. 31, 171–186.
Vorlicek, T.P., Kahn, M.D., Kasuya, Y., Helz, G.R., 2004. Capture of molybdenum in pyrite-forming sediments: role of ligand-induced reduction by polysulfides. Geochem. Cosmochim. Acta 68, 547–556.
Wanty, R.B., 1986. Geochemistry of Vanadium in an Epigenetic Sandstone-hosted Vanadium-uranium Deposit, Henry Basin Utah. Ph.D. thesis. Colorado School of Mines, Golden, Colorado.
Wanty, R.B., Goldhaber, M.B., 1992. Thermodynamics and kinetics of reactions involving vanadium in natural systems – accumulation of vanadium in sedimentary rocks. Geochem. Cosmochim. Acta 56 (4), 1471–1483.
Webster, J.G., 1990. The solubility of As_2S_3 and speciation of as in dilute and sulphide-bearing fluids at 25 and 90°C. Geochem. Cosmochim. Acta 54, 1009–1017.
Wehrli, B., Stumm, W., 1989. Vanadyl in natural waters – adsorption and hydrolysis promote oxygenation. Geochem. Cosmochim. Acta 53 (1), 69–77.
Wesolowski, D.J., Drummond, S.E., Mesmer, R.E., Ohomoto, H., 1984. Hydrolysis equilibria of tungsten(VI) in aqueous sodium Chloride solutions to 300 C. Inorg. Chem. 23, 1120–1132.
Wilkie, J.A., Hering, J.G., 1998. Rapid oxidation of geothermal arsenic(III) in streamwaters of the eastern sierra Nevada. Environ. Sci. Technol. 32, 657–662.
Wilkin, R.T., Ford, R.G., 2006. Arsenic solid-phase partitioning in reducing sediments of a contaminated wetland. Chem. Geol. 228, 156–174.
Windom, H.L., Schropp, S.J., Calder, F.D., Ryan, J.D., Smith Jr., R.G., Burney, L.C., Rawlinson, C.H., 1989. Natural trace metal concentrations in estuarine and coastal marine sediments of the southeastern United States. Environ. Sci. Technol. 23 (3), 314–320.
Wolthers, M., Charlet, L., van der Weijden, C., van der Linde, P.R., Rickard, D., 2005. Arsenic mobility in the ambient sulfidic environment: sorption of arsenic(V) and arsenic(III) onto disordered mackinawite. Geochem. Cosmochim. Acta 69 (14), 3483–3492.
Wright, M.T., Belitz, K., 2010. Factors controlling the regional distribution of vanadium in groundwater. Ground Water 48 (4), 515–525.
Wright, M.T., Stollenwerk, K.G., Belitz, K., 2014. Assessing the solubility controls on vanadium in groundwater, northeastern San Joaquin Valley, CA. Appl. Geochem. 48, 41–52.
Yang, N.F., Welch, K.A., Mohajerin, T.J., Telfeyan, K., Chevis, D.A., Grimm, D.A., Lyons, W.B., White, C.D., Johannesson, K.H., 2015. Comparison of arsenic and molybdenum geochemistry in meromictic lakes of the McMurdo Dry Valleys, Antarctica: implications for oxyanion-forming trace element behavior in permanently stratified lakes. Chem. Geol. 404, 110–125.
Yeghicheyan, D., Carignan, J., Valladon, M., Bouhnik le Coz, M., Le Cornec, F., Castrec-Rouelle, M., Robert, M., Aquilina, L., Aubry, E., Churlaud, C., Dia, A., Deberdt, S., Dupré, B., Freydier, R., Gruau, G., Hénin, O., de Kersabiec, A., Macé, J., Marin, L., Morin, N., Petitjean, P., Serrat, E., 2001. A compilation of silicon and thirty one trace elements measured in natural river water reference material SLRS-4 (NRC-CNRC). Geostand. Newsl. 25, 465–474.
Zaback, D.A., Pratt, L.M., 1992. Isotopic composition and speciation of sulfur in the Miocene Monterey Formation, Re- evaluation of sulfur reaction during early diagenesis in marine environments. Geochem. Cosmochim. Acta 56, 763–774.